nature structural & molecular biology

ARTICLES

https://doi.org/10.1038/s41594-019-0211-4

Mechanism for recycling tRNAs on stalled ribosomes

Matthew C. J. Yip, Alexander F. A. Keszei, Qing Feng, Vincent Chu, Michael J. McKenna and Sichen Shao*

Aberrantly stalled ribosomes initiate the ribosome-associated quality control (RQC) and mRNA surveillance pathways for the degradation of potentially toxic peptides and faulty mRNAs. During RQC, ANKZF1 (yeast Vms1p) releases ubiquitinated nascent proteins from 60S ribosomal subunits for proteasomal degradation. Here, we use a cell-free system to show that ANKZF1 and Vms1p sever polypeptidyl-tRNAs on RQC complexes by precisely cleaving off the terminal 3′CCA nucleotides universal to all tRNAs. This produces a tRNA fragment that cannot be aminoacylated until its 3′CCA end is restored. The recycling of ANKZF1-cleaved tRNAs is intact in the mammalian cytosol via a two-step process that requires the removal of a 2′,3′-cyclic phosphate and TRNT1, the sole CCA-adding enzyme that mediates tRNA biogenesis in eukaryotes. TRNT1 also discriminates between properly folded tRNA substrates and aberrant tRNA substrates, selectively tagging the latter for degradation. Thus, ANKZF1 liberates peptidyl-tRNAs from stalled ribosomes such that the tRNA is checked in an obligate way for integrity before reentry into the translation cycle.

Ribosomes may stall during protein synthesis due to mutated, misprocessed or damaged translational components. Failing to rescue or eliminate stalled translation complexes is associated with proteotoxicity and neurodegeneration[1–3]. Ribosomes that stall on aberrant non-stop or no-go mRNAs initiate dedicated mRNA surveillance mechanisms[4–8] and the evolutionarily conserved RQC pathway[9–11] for degradation of the mRNAs and incompletely synthesized nascent proteins associated with stalled ribosomes, respectively. This simultaneously eliminates potentially dominant negative peptides and the risk of defective mRNAs causing future translational stalls.

RQC and non-stop or no-go mRNA surveillance rely on Hbs1L (HBS1-like protein; yeast Hbs1p) and Pelota (Dom34p), which function with ABCE1 (ATP-binding cassette sub-family E member 1; Rli1p) to dissociate stalled 80S ribosomes into 40S and 60S ribosomal subunits[4,10,12]. This ribosome-splitting step traps the nascent polypeptidyl-tRNA in the 60S ribosomal subunit[4,9,10], producing a 60S–peptidyl-tRNA complex that is completely distinct from normal translation intermediates. During RQC, NEMF (nuclear export mediator factor; Rqc2p) selectively binds the unique 60S–peptidyl-tRNA interface and stabilizes the complex by preventing 40S subunits from rejoining[13–15]. This promotes recruitment of the E3 ubiquitin ligase Listerin (Ltn1p) to ubiquitinate the nascent protein[11,13,14].

Subsequently, the ubiquitinated nascent protein must be extracted from the 60S ribosomal subunit for proteasomal degradation. The AAA+ ATPase p97 (Cdc48p) and its ubiquitin-binding cofactors Ufd1p–Npl4p (ubiquitin fusion degradation protein 1 and nuclear protein localization protein 4) are implicated in this extraction reaction[9,16,17]. TCF25 (transcription factor 25; Rqc1p) also associates with the 60S–RQC complex, where it may regulate Listerin-mediated ubiquitination and p97 recruitment[9,18–20]. If nascent peptide ubiquitination and extraction from the 60S fails to occur, then studies in yeast have shown that Rqc2p can catalyze the mRNA-free addition of C-terminal alanines and threonines (CAT tails) to the nascent protein[14,19]. CAT tailing can expose lysine residues for ubiquitination[21] but is also linked to aggregation and proteotoxicity[2,22,23].

Recent studies demonstrated that ANKZF1 (ankyrin repeat and zinc finger domain-containing protein 1; Vms1p), another putative Cdc48p cofactor[24], directly releases nascent proteins from RQC complexes[20,25,26]. Vms1p is genetically linked to RQC factors in protecting cells from translational stress; deleting Vms1p results in the accumulation of RQC substrates, resembling the phenotype of deleting the RQC ubiquitin ligase Ltn1p[22,25,26]. Two studies initially proposed that Vms1p hydrolyzes the ester bond between tRNA and nascent protein, similar to how the release factor eRF1 (eukaryotic release factor 1) liberates nascent proteins during translation termination. Indeed, ANKZF1 and Vms1p have an eRF1-like domain with conserved sequences similar to the catalytic Gly-Gly-Gln (GGQ) motif of eRF1 required for peptide hydrolysis; mutating these residues in ANKZF1 or Vms1p impairs nascent chain (NC) release[25,26]. However, a subsequent study showed that ANKZF1 instead acts as an endonuclease on peptidyl-tRNA to release ubiquitinated proteins[20]. This study proposed that ANKZF1 cleaves off four nucleotides from the 3′ end of peptidyl-tRNA based on the migration of the cleaved fragment on sequencing gels, although the purpose of this nucleolytic mechanism remains unclear.

In contrast to mRNAs and nascent proteins, we have only limited understanding of how other components of stalled translation complexes, such as tRNAs and the ribosomal subunits, are processed. Using a mammalian cell-free system, we show that ANKZF1 and Vms1p selectively cleave off the three 3′ terminal CCA nucleotides universal to all tRNAs. ANKZF1 cleavage generates a tRNA fragment that cannot be used for translation unless the 3′CCA end is restored. In eukaryotes, a single enzyme, TRNT1 (tRNA nucleotidyl transferase 1) posttranscriptionally adds the invariant CCA sequence to the 3′ ends of all cytoplasmic and mitochondrial tRNAs[27]. TRNT1 also discriminates between properly and misfolded tRNAs to selectively tag the latter for degradation[28]. We show that the recycling of ANKZF1-cleaved tRNAs, but not that of tRNAs lacking four 3′ nucleotides, is intact in the mammalian cytosol via a two-step process requiring the removal of a terminal 2′,3′-cyclic phosphate and TRNT1. Thus, ANKZF1 releases peptidyl-tRNAs from stalled ribo-

Department of Cell Biology, Harvard Medical School, Boston, MA, USA. *e-mail: sichen_shao@hms.harvard.edu

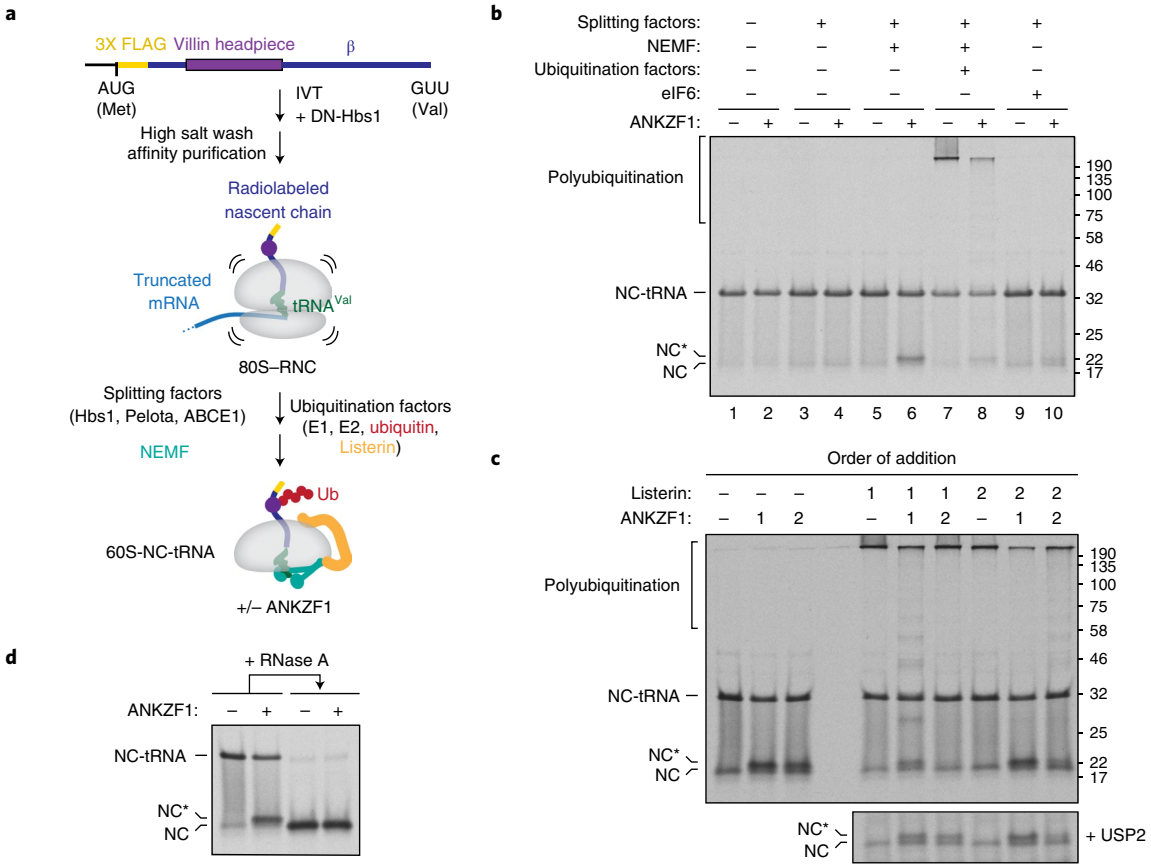

Fig. 1 | ANKZF1 severs nascent polypeptidyl-tRNAs on 60S–RQC complexes. a, Scheme for reconstituting ANKZF1 activity on stalled 80S ribosome–nascent protein complexes (RNCs) with purified factors. In vitro translation (IVT) reactions were (1) initiated of a construct encoding an N-terminal 3X Flag epitope tag, the fast-folding villin headpiece domain and a portion of Sec61β truncated at valine (residue 68 of endogenous Sec61β)[10], (2) supplemented with DN-Hbs1 after 7 min (ref. [29]) and (3) allowed to proceed to 25–30 min. Reactions were centrifuged over a high-salt sucrose cushion to isolate ribosomes and substrate RNCs were affinity-purified via the 3X Flag tag[29]; 5 nM of purified 80S RNCs were incubated with an energy-regenerating system, splitting factors (50 nM Hbs1, 50 nM Pelota, 100 nM ABCE1), ubiquitination factors (75 nM E1, 250 nM E2, 10 μM ubiquitin, 5 nM Listerin), 10 nM NEMF[13] and 25 nM ANKZF1 as indicated at 32 °C for 15 min. **b**, SDS–PAGE and autoradiography analysis of reconstituted ANKZF1 reactions. tRNA-associated (NC-tRNA), ANKZF1-cleaved (NC*), unmodified (NC) and polyubiquitinated nascent chain is indicated. **c**, Reactions as in **b** in which the addition of Listerin and/or ANKZF1 was immediate (1) or delayed by 15 min (2). Total reactions (30 min) were analyzed directly (top) or after deubiquitination by the catalytic domain of USP2 (bottom). **d**, Treating ANKZF1 cleavage reactions with RNase A collapses the size of ANKZF1-cleaved nascent chain (NC*) to that of the unmodified nascent chain (NC). All experiments are representative of at least three independent replications. Uncropped gel images are shown in Supplementary Fig. 1c and Supplementary Dataset 1.

somes to generate tRNA intermediates that are obligately rechecked for quality while being recycled for translation.

Results

Reconstitution of ANKZF1 activity on RQC complexes with purified factors. To dissect ANKZF1 function, we reconstituted its activity with purified factors. We generated stalled ribosome–nascent protein complexes (RNCs) in a mammalian cell-free translation system programmed with a truncated mRNA that initiates RQC[10]. Shortly after initiating the translation reaction, we added dominant negative Hbs1L (DN-Hbs1) deficient in GTPase activity to prevent RNC splitting. We then salt-stripped and affinity-purified the 80S RNCs via an N-terminal epitope tag encoded in the radiolabeled nascent protein[29] (Fig. 1a). The purified 80S RNCs were directly incubated with or without wild-type ribosome-splitting factors, ubiquitination factors, NEMF and ANKZF1, thereby reconstituting RQC events starting with ribosome dissociation[13].

ANKZF1 severance of nascent chain–tRNA (NC-tRNA) on stalled RNCs required ribosome splitting and NEMF, which directly binds peptidyl-tRNA at the 60S ribosomal subunit interface[13,14] (Fig. 1b, lane 6, and Supplementary Figs. 1–3). ANKZF1 was only weakly active on 60S–NC-tRNA complexes stabilized by eukaryotic translation initiation factor 6 (eIF6), a ribosome biogenesis factor that also prevents 40S rejoining but does not contact peptidyl-tRNA[13,14,29,30] (Fig. 1b, lane 10 and Supplementary Fig. 3b). ANKZF1 was also completely inactive against NC-tRNAs that 'slip out' of 60S ribosomal subunits[10,29] (Supplementary Fig. 3c), demonstrating a requirement for the 60S ribosomal subunit. Thus, ANKZF1 selectively severs NC-tRNAs stabilized by NEMF on 60S ribosomal subunits[20], mirroring the precise requirements for efficient Listerin-mediated ubiquitination during RQC[13,29] (Fig. 1b, lane 7).

ANKZF1 decreased the length of polyubiquitin chains on the nascent protein when added before or together with Listerin (Fig. 1b,c and Supplementary Figs. 1–3). This reduction is a consequence of Listerin's function strictly on 60S–RNCs but not on released nascent chains[9,10,20]. Hence, ANKZF1 had no effect on ubiquitination if added after Listerin (Fig. 1c). The ubiquitination status of the RNC neither stimulates nor impairs ANKZF1 activity. Nevertheless, the complete system produced essentially no released nascent chains that were not ubiquitinated, suggesting that ANKZF1 acts

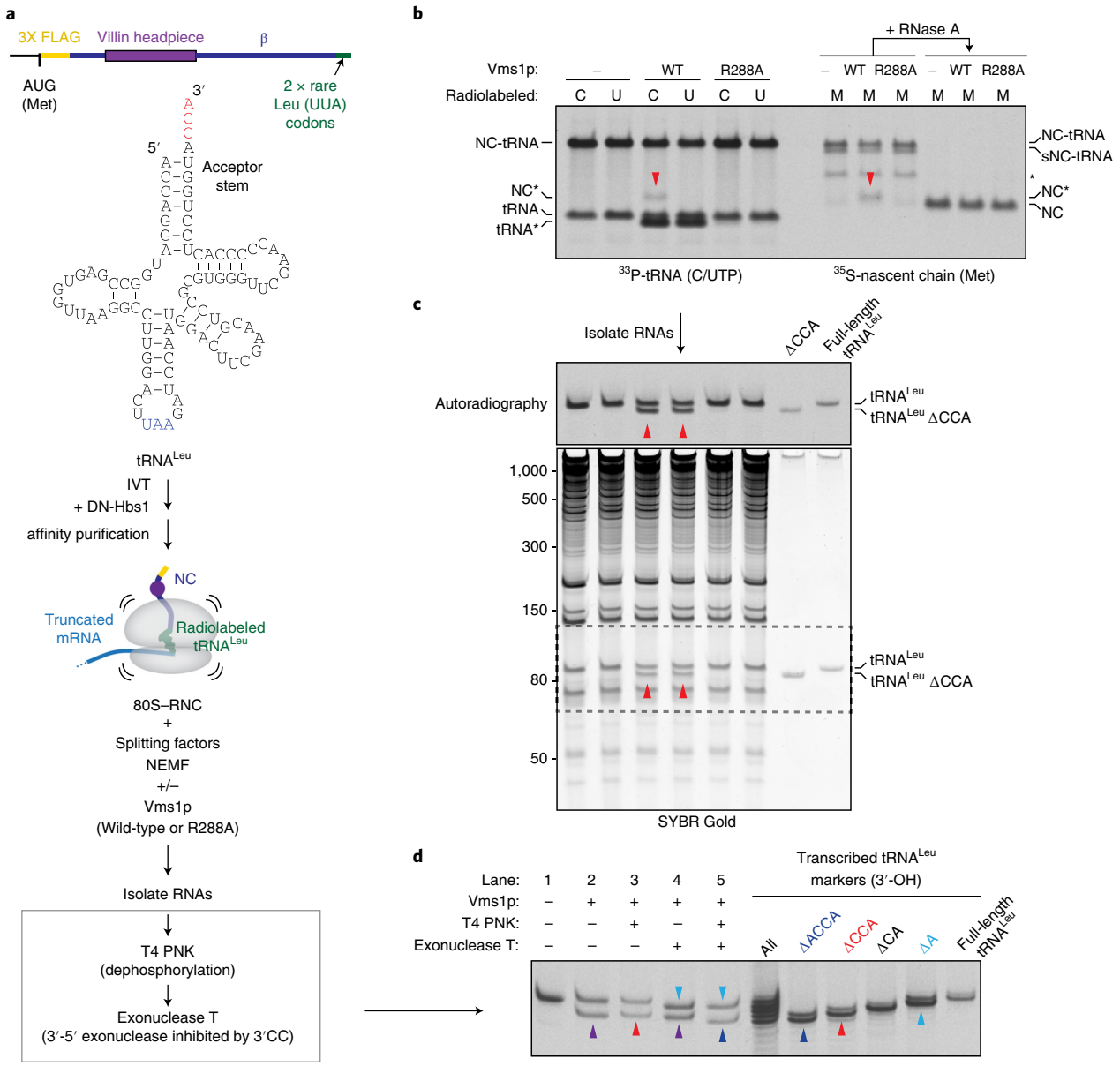

Fig. 2 | ANKZF1 (yeast Vms1p) cleaves off the 3′CCA of peptidyl-tRNAs. a, Scheme for incorporating radiolabeled tRNA^{Leu} into RNCs. IVT reactions of an mRNA truncated at two rare UUA leucyl codons were performed and purified as shown in Fig. 1a. Where applicable, transcribed tRNA^{Leu} with the UAA anticodon was included during translation. **b**, 10 nM RNCs containing peptidyl-tRNA^{Leu} uniformly radiolabeled with cytidine (C) or uridine (U) nucleotides (left), or radiolabeled nascent protein (M, right), were incubated with splitting factors, NEMF and 125 nM wild-type (WT) or catalytically inactive (R288A) Vms1p. Reactions were analyzed using NuPAGE and autoradiography. Radiolabeled Vms1p cleavage products (NC*, red arrowhead and tRNA*) are indicated. NC-tRNA, full-length polypeptidyl-tRNA; sNC-tRNA, short polypeptidyl-tRNA generated by ribosome stalling at the first rare leucyl codon; * (right margin), NC-RNA species possibly generated by the incorporation of mitochondrial tRNAs. **c**, RNAs extracted from the reactions in **b** were analyzed by TBE–urea–PAGE and autoradiography (top) or SYBR Gold staining (bottom). The red arrowheads denote Vms1p-cleaved tRNA fragments. **d**, RNAs isolated from the Vms1p cleavage reactions were treated with or without 0.12 U µl^{-1} T4 PNK followed by 0.05 U µl^{-1} exonuclease T. Migration of tRNA^{Leu} containing a 3′OH and lacking one (ΔA, light blue), three (ΔCCA, red) or four (ΔACCA, dark blue) 3′ terminal nucleotides is indicated. The purple arrows indicate migration of ΔCCA tRNA^{Leu} with a 2′,3′-cyclic phosphate produced by Vms1p cleavage. Experiments are representative of at least three independent replications. Uncropped gel images are shown in Supplementary Dataset 1.

sufficiently slowly to ensure Listerin-mediated ubiquitination before releasing nascent proteins from the 60S.

ANKZF1 cleaves peptidyl-tRNAs on 60S–RQC complexes. One possibility for how ANKZF1 releases NC-tRNA is by hydrolyzing the ester bond between the nascent chain and tRNA[25,26], similar to the mechanism eRF1 uses during translation termination. However, arguing against this is the observation that ANKZF1 and yeast Vms1p both generate a nascent protein product (NC*) approximately 1–2 kDa larger than the molecular weight of the nascent chain (NC)[20] (Fig. 1b–d and Supplementary Fig. 4). In comparison, treating RNCs with RNase A to degrade tRNA, or with puromycin to break the NC-tRNA ester bond at the ribosomal peptidyl transferase center, generated NC-sized products (Supplementary Fig. 4c). The extra weight of the ANKZF1-cleaved nascent protein product (NC*) is probably contributed by a portion of the 3′ end of the tRNA attached

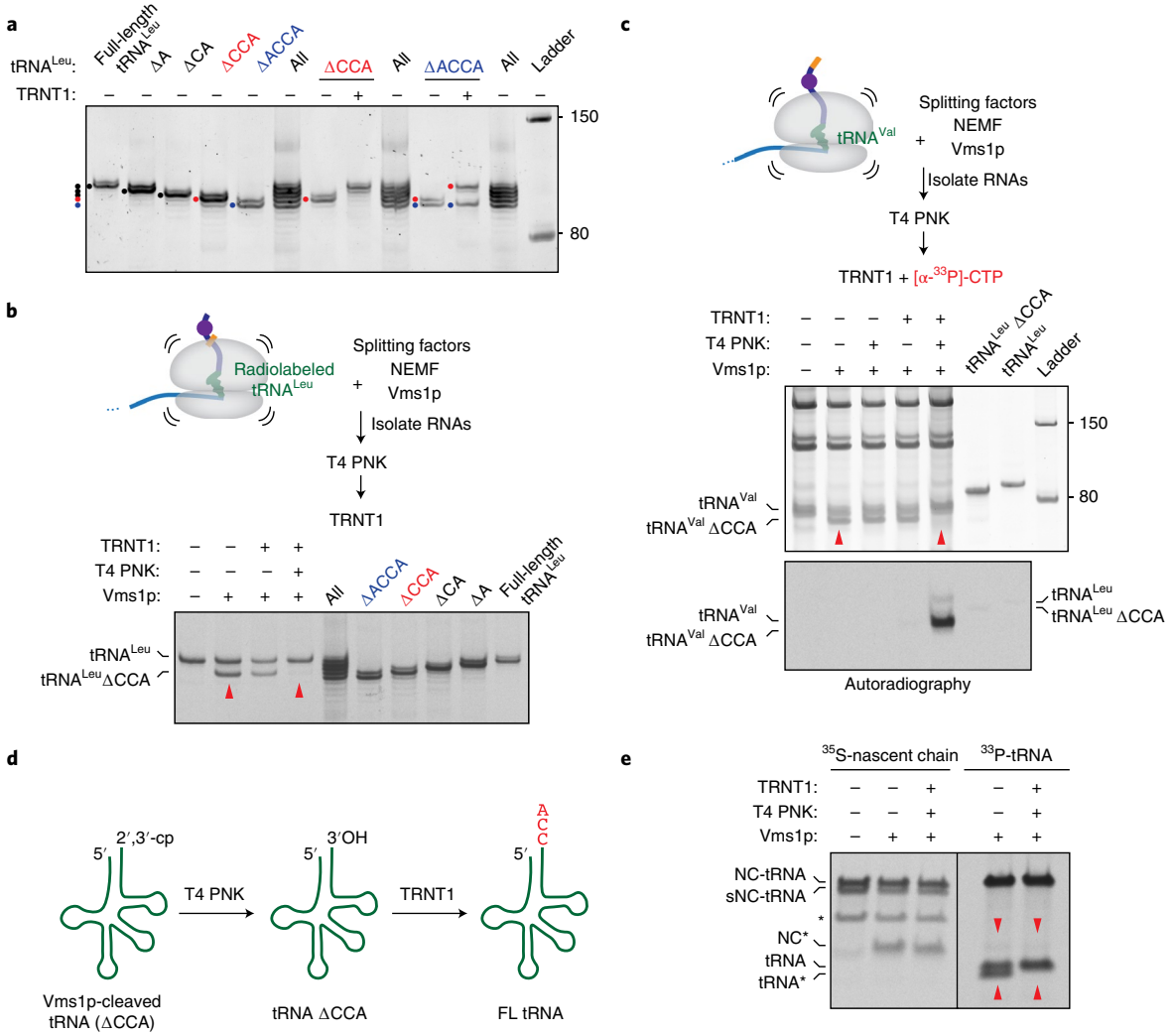

Fig. 3 | TRNT1 recycles Vms1p-cleaved tRNAs after 2′,3′-dephosphorylation. a, Transcribed tRNA^{Leu} lacking the indicated terminal 3′ nucleotides (Δ) was incubated with or without 100 nM TRNT1 and analyzed by TBE–urea–PAGE and SYBR Gold staining. Migration of unmodified and TRNT1-modified products of ΔCCA (red dots) or ΔACCA (blue dots) tRNA^{Leu} are indicated. Unmodified full-length and serially 3′-truncated tRNA^{Leu} transcripts were loaded as size markers (left). The upper bands are minor heterogeneous products of transcription. **b**, RNAs isolated from Vms1p cleavage reactions of RNCs with radiolabeled peptidyl-tRNA^{Leu} were treated with 0.12 U μl^{-1} T4 PNK and/or 100 nM TRNT1, demonstrating the production and repair of Vms1p-cleaved tRNAs. **c**, RNAs isolated from Vms1p cleavage reactions of non-radiolabeled RNCs containing endogenous peptidyl-tRNA^{Val} (as in Fig. 1a) were treated with T4 PNK and TRNT1 in the presence of [α-^{33}P]-CTP to detect specific cytidine addition. **d**, Scheme for recycling of ANKZF1- or Vms1p-cleaved tRNAs by T4 PNK and TRNT1. **e**, 10 nM RNCs with radiolabeled nascent protein or peptidyl-tRNA^{Leu} were incubated with splitting factors, NEMF and Vms1p, with or without 0.12 U μl^{-1} T4 PNK and 100 nM TRNT1, and directly analyzed by NuPAGE and autoradiography. NC-tRNA, Vms1p-released nascent protein (NC*), Vms1p-cleaved tRNA* and full-length tRNA are indicated. The red arrowheads denote the generation and repair of Vms1p products. Experiments are representative of at least three independent replications. Uncropped gel images are shown in Supplementary Dataset 1.

to the NC. Consistent with this, RNase A treatment reduced the size of NC* to that of NC (Fig. 1d). This supports the designation that ANKZF1 acts as a ribonuclease to cleave peptidyl-tRNA[20].

To directly test if ANKZF1 and Vms1p cleave peptidyl-tRNA, we incorporated a radiolabeled leucyl-tRNA (tRNA^{Leu}) into RNCs stalled at a rare UUA leucine codon (Fig. 2a and Supplementary Figs. 5 and 6). We used these RNCs in reconstituted reactions with splitting factors, NEMF and yeast Vms1p, which we could add at higher concentrations to improve cleavage efficiency (Supplementary Fig. 4a,b). NC* contained a radiolabel when tRNA^{Leu} was produced with ^{33}P-labeled CTP, but not when it was produced with ^{33}P-labeled UTP (Fig. 2b and Supplementary Fig. 6a–d), indicating that a portion of tRNA^{Leu} containing cytidine, but not uridine, remains attached to the nascent protein after Vms1p cleavage. The remaining 5′ tRNA fragment was approximately the size of transcribed tRNA^{Leu} lacking the 3′CCA nucleotides universal to all tRNAs (Fig. 2b,c). As expected (Fig. 1b), Vms1p did not cleave free tRNA^{Leu} (Supplementary Fig. 6e).

ANKZF1 precisely cleaves off the 3′CCA of tRNAs and leaves a 2′,3′-cyclic phosphate. Next, we characterized and mapped the Vms1p cleavage site. While transcribed tRNAs have a 3′ hydroxyl group, all known metal-ion-independent ribonucleases generate RNA fragments with a 2′,3′-cyclic phosphate[31]. To differentiate between these possibilities, we treated Vms1p-cleaved tRNAs with T4 polynucleotide kinase (T4 PNK), which can dephosphorylate 2′,3′-cyclic phosphates[32–34]. To map the cleavage site, we used exonuclease T, a 3′–5′ single-stranded ribonuclease that is inhibited by consecutive cytidines[35]. As expected, exonuclease T removed

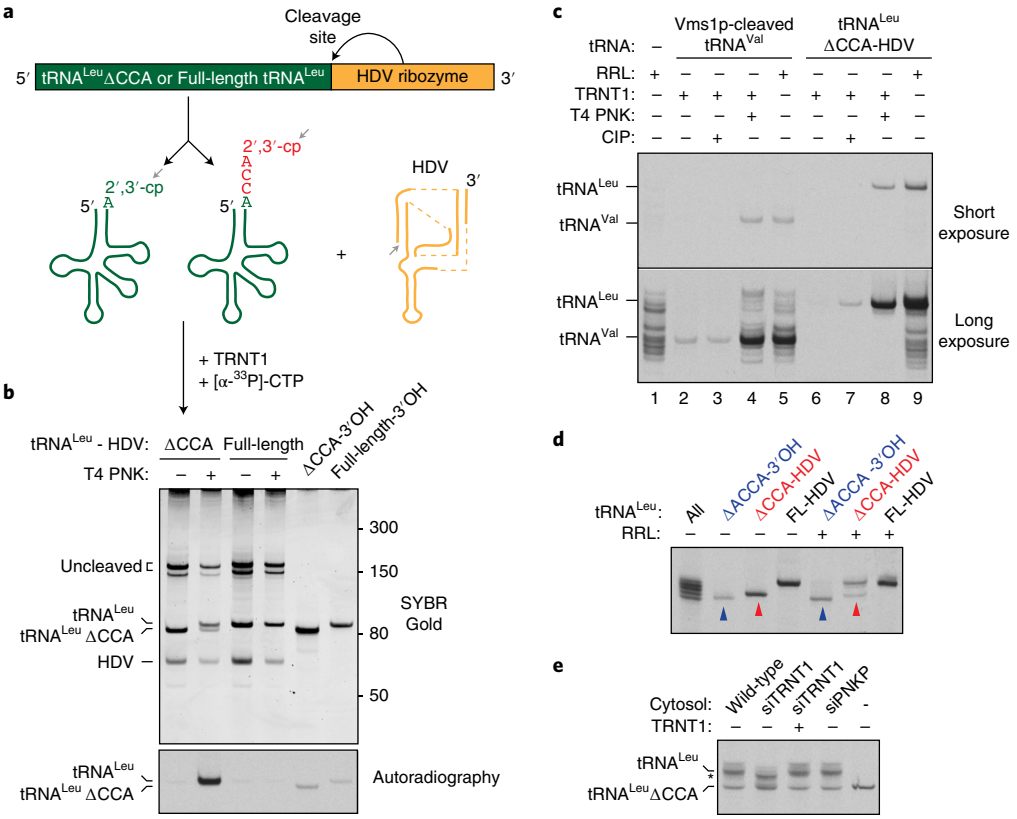

Fig. 4 | tRNA recycling is intact in the mammalian cytosol. a, Scheme of self-cleaving 3′ HDV ribozyme constructs that generate full-length (FL-HDV) $tRNA^{Leu}$ or $tRNA^{Leu}$ lacking the 3′CCA (ΔCCA-HDV) with a homogenous 2′,3′-cyclic phosphate end. **b**, ΔCCA-HDV or FL-HDV were treated with 0.12 U µl^{-1} T4 PNK and 100 nM TRNT1 in the presence of [α-^{33}P]-CTP and analyzed by TBE–urea–PAGE and SYBR Gold staining (top) or autoradiography (bottom). **c**, Vms1p-cleaved $tRNA^{Val}$ (left) or ΔCCA-HDV (right) were incubated with 0.2 U µl^{-1} CIP, which can remove 3′-phosphates but not 2′,3′-cyclic phosphates[19], or 0.12 U µl^{-1} T4 PNK, followed by 100 nM TRNT1 or RRL in the presence of [α-^{33}P]-CTP to detect CCA addition. Short and long autoradiography exposures are shown to demonstrate signal-to-noise ratio relative to background labeling. **d**, FL-HDV, ΔCCA-HDV or exonuclease-treated transcribed $tRNA^{Leu}$ lacking four 3′ nucleotides (ΔACCA, blue arrow) were incubated with or without RRL. **e**, Radiolabeled ΔCCA-HDV was incubated with cytosolic lysate extracted from HEK293T cells treated with a negative control siRNA (wild-type) or siRNAs targeting TRNT (siTRNT) or PNKP (siPNKP), with or without recombinant TRNT1. Knocking down TRNT1 results in unrepaired tRNA intermediates (*). Experiments are representative of at least three independent replications. Uncropped gel images are shown in Supplementary Dataset 1.

a single base from full-length $tRNA^{Leu}$ (Fig. 2d, lanes 4 and 5, and Supplementary Fig. 7a, lane 2), coinciding with the terminal adenine of the 3′CCA. T4 PNK did not alter full-length $tRNA^{Leu}$, but slightly shifted Vms1p-cleaved products to a higher apparent molecular weight (Fig. 2d, lane 3). This is consistent with observations that a negatively charged 2′,3′-cyclic phosphate causes RNAs to run faster during gel electrophoresis[33].

Exonuclease T removed an additional nucleotide from Vms1p-cleaved tRNA fragments only after T4 PNK dephosphorylation (Fig. 2d, lane 5). This coincides with the single non-base-paired discriminator nucleotide immediately preceding the 3′CCA of $tRNA^{Leu}$ (Fig. 2a and Supplementary Fig. 7a) and further supports the assignment that Vms1p generates a 2′,3′-cyclic phosphate that must be resolved to hydroxyl groups before exonuclease T can act. A recent study suggested that ANKZF1 removes four nucleotides[20], which likely reflects the different migrations of 2′,3′-cyclic phosphate and 3′ hydroxyl species on sequencing gels[33]. Our results show that mammalian ANKZF1 and yeast Vms1p selectively cleave off the 3′CCA of peptidyl-tRNAs on 60S ribosomal subunits. Because all tRNAs end with an invariant 3′CCA[27], ANKZF1 cleavage would be compatible with ribosome stalling at any codon. Supporting this idea is our and others' observations of ANKZF1 and Vms1p activity on multiple substrates[20,25,26] (Figs. 1 and 2 and Supplementary Fig. 7).

TRNT1 recycles ANKZF1-cleaved tRNAs after removal of the 2′3′-cyclic phosphate. Vms1p releases tRNAs from ribosomal complexes (Supplementary Fig. 7b) that would not be functional for translation unless the 3′CCA is added back. It is possible that these tRNA products are a waste product of RQC. Alternatively, they may be recycled to reenter the translation cycle. In eukaryotes, a single enzyme, TRNT1, adds the 3′CCA to all cytoplasmic and mitochondrial tRNAs during tRNA biosynthesis[27,36] (Supplementary Fig. 7c). TRNT1 also mediates tRNA quality control by tagging acceptor stem–destabilized tRNAs or tRNA-like structures with tandem CCA repeats, which serve as a signal for degradation[28]. By precisely removing the 3′CCA of peptidyl-tRNAs on stalled ribosomes, Vms1p-cleaved tRNAs may be substrates for recycling and quality control by TRNT1.

To test this hypothesis, we purified human TRNT1 lacking the N-terminal mitochondrial transit peptide[36] (Supplementary Fig. 7d). As expected, recombinant TRNT1 added or repaired the 3′CCA on transcribed tRNAs that contain a 3′ hydroxyl group lacking up to three, but not four, 3′ nucleotides (Fig. 3a and Supplementary Fig. 7a,e). TRNT1 also modified Vms1p-cleaved tRNAs only after T4 PNK treatment to remove the 2′,3′-cyclic phosphate (Fig. 3b–d and Supplementary Fig. 7b). The same results were seen with tRNAs cleaved by mammalian ANKZF1 (Supplementary Fig. 7f,g). Adding TRNT1 and T4 PNK directly to the Vms1p cleavage reactions of stalled RNCs was sufficient to repair Vms1p-cleaved tRNAs

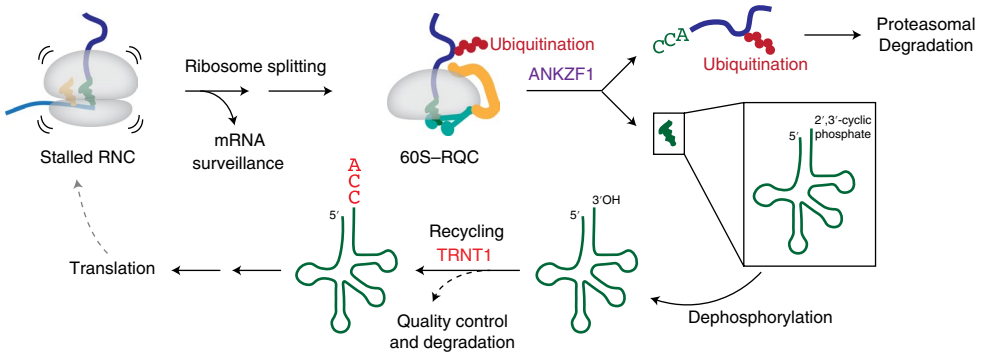

Fig. 5 | Working model for recycling tRNAs on stalled ribosomes. A stalled RNC is split into 60S and 40S ribosomal subunits by factors implicated in mRNA surveillance. The unique 60S–nascent peptidyl–tRNA complex is recognized by the RQC factors NEMF (teal) and Listerin (orange), which ubiquitinates the nascent protein. ANKZF1 specifically acts on this complex to cleave off the 3′CCA of the peptidyl-tRNA. This releases ubiquitinated nascent proteins still attached to the CCA residues for proteasomal degradation and generates a tRNA lacking the 3′CCA and ending with a 2′,3′-cyclic phosphate. After removal of the cyclic phosphate moiety, ANKZF1-cleaved tRNA products can be recycled by TRNT1. TRNT1 adds back the 3′CCA nucleotides and queries the integrity of the tRNA to potentially tag aberrant tRNAs for degradation. Recycled tRNAs with an intact 3′CCA can then be aminoacylated and reused for translation.

without impairing NC* generation (Fig. 3e and Supplementary Fig. 7h). This indicates that ANKZF1 and Vms1p simultaneously produce tRNA recycling intermediates while releasing ubiquitinated nascent proteins for degradation.

Recycling of ANKZF1-cleaved tRNAs is intact in the mammalian cytosol. To detect tRNA recycling independently of upstream events, we developed a substrate to assay recycling in crude extracts. We transcribed $tRNA^{Leu}$ constructs containing a 3′ hepatitis delta virus (HDV) ribozyme that cleaves 5′ of itself to produce a homogenous 2′,3′-cyclic phosphate[33] (Fig. 4a and Supplementary Fig. 8a). Like Vms1p-cleaved tRNAs, tRNA-HDV lacking the 3′CCA (ΔCCA-HDV) strictly required T4 PNK dephosphorylation for CCA addition by TRNT1 (Fig. 4b,c and Supplementary Fig. 8b). Notably, rabbit reticulocyte lysate (RRL) and human embryonic kidney 293 (HEK293) or HEK293T cytosolic lysates efficiently repaired both Vms1p-cleaved tRNAs and ΔCCA-HDV (Fig. 4c,d and Supplementary Fig. 8c,d). This indicates that tRNA recycling is intact in the mammalian cytosol.

After tRNA recycling, ΔCCA-HDV should be functional for translation. Consistent with this prediction, ΔCCA-HDV rescued ribosome stalling at rare UUA leucine codons[37] (Supplementary Fig. 8e) and was incorporated into RNCs ending in the UUA codon in cell-free translations (Supplementary Fig. 8f). This confirms a mechanism that permits CCA addition, aminoacylation and usage during translation. Compared to RRL, HEK lysates heterogeneously modified both ΔCCA and full-length tRNA-HDV (Fig. 4d,e and Supplementary Fig. 8g,h). These products may represent the addition of extra nucleotides or posttranscriptional RNA modifications. Nonetheless, knocking down TRNT1 diminished tRNA recycling by HEK293T lysates; this was specifically rescued by adding back recombinant TRNT1 (Fig. 4e and Supplementary Fig. 8i). This verifies the requirement for TRNT1 in this tRNA recycling pathway.

Discussion

Our results demonstrate that ANKZF1 (and yeast Vms1p) specifically cleaves off the universal 3′CCA of peptidyl-tRNAs on 60S ribosomal subunits undergoing RQC. ANKZF1 activity liberates ubiquitinated nascent proteins for degradation and generates a tRNA intermediate that can be recycled or targeted for degradation by TRNT1 (Fig. 5). This tRNA recycling pathway complements RQC mechanisms[4,6,9,11] that surveil and degrade the mRNAs and nascent proteins associated with stalled ribosomes. We posit that cells have evolved mechanisms to systematically check the integrity of each translational component that may cause aberrant ribosome stalling and avoid wasting functional translational factors.

Recycling of ANKZF1-cleaved tRNAs occurs through a two-step process that proceeds through a 2′,3′-cyclic phosphate intermediate before CCA is added. The 2′,3′-cyclic phosphate may provide protection from degradation[38], such that ANKZF1-cleaved intermediates are essentially inert tRNAs that cannot participate in translation until both recycling steps are successful. Exactly how this 2′,3′-cyclic phosphate is removed remains unclear, similar to our limited understanding of how these ends are resolved in other physiological processes such as ribosomal RNA biogenesis[39]. Knocking down the closest mammalian homolog to T4 PNK, polynucleotide kinase-3′-phosphatase (PNKP), which is implicated in DNA repair[40,41], had no effect on tRNA recycling (Fig. 4e). It is likely that a dedicated factor that resolves the 2′,3′-cyclic phosphate on ANKZF1-cleaved tRNA fragments remains to be identified. This intermediate reaction may confer an additional quality control checkpoint, which interfaces with enzymes that mediate RNA degradation or additional endonucleolytic cleavages. Alternatively, it is possible that multiple redundant conditions can remove this 2′,3′-cyclic phosphate.

This recycling mechanism differs from tRNA biosynthesis, in which cleavage of 3′ trailers of tRNA precursors directly generates a 3′ hydroxyl group for 3′CCA addition by TRNT1[42], and tRNA splicing, in which ligases directly act on or modify 2′,3′-cyclic phosphates[43,44]. TRNT1 is also implicated in the repair of mature tRNAs lacking all or portions of the 3′CCA, although how these substrates are generated in eukaryotes is poorly understood[45]. During oxidative stress, the mammalian endonuclease angiogenin primarily cleaves the anticodon stem-loops of tRNAs[46–48] but may also acutely remove the 3′ terminal adenine from free tRNAs that can be repaired by TRNT1[34]. This contrasts with the precise removal of the entire 3′CCA by ANKZF1 and Vms1p on RQC complexes. Finally, our findings linking RQC with tRNA recycling and quality control raises the speculation that certain types of tRNA defects may induce ribosome stalling. The types of tRNA aberrancies that may initiate these quality-control pathways, as well as detailed molecular mechanisms that may query the subunits of stalled ribosomes[49], remain the focus of future investigations.

Online content

Any methods, additional references, Nature Research reporting summaries, source data, statements of data availability and associated accession codes are available at https://doi.org/10.1038/s41594-019-0211-4.

Received: 24 January 2019; Accepted: 6 March 2019;
Published online: 22 April 2019

References

1. Chu, J. et al. A mouse forward genetics screen identifies LISTERIN as an E3 ubiquitin ligase involved in neurodegeneration. *Proc. Natl Acad. Sci. USA* **106**, 2097–2103 (2009).
2. Choe, Y.-J. et al. Failure of RQC machinery causes protein aggregation and proteotoxic stress. *Nature* **531**, 191–195 (2016).
3. Ishimura, R. et al. Ribosome stalling induced by mutation of a CNS-specific tRNA causes neurodegeneration. *Science* **345**, 455–459 (2014).
4. Shoemaker, C. J., Eyler, D. E. & Green, R. Dom34:Hbs1 promotes subunit dissociation and peptidyl-tRNA drop-off to initiate no-go decay. *Science* **330**, 369–372 (2010).
5. Shoemaker, C. J. & Green, R. Translation drives mRNA quality control. *Nat. Struct. Mol. Biol.* **19**, 594–601 (2012).
6. Doma, M. K. & Parker, R. Endonucleolytic cleavage of eukaryotic mRNAs with stalls in translation elongation. *Nature* **440**, 561–564 (2006).
7. van Hoof, A., Frischmeyer, P. A., Dietz, H. C. & Parker, R. Exosome-mediated recognition and degradation of mRNAs lacking a termination codon. *Science* **295**, 2262–2264 (2002).
8. Frischmeyer, P. A. et al. An mRNA surveillance mechanism that eliminates transcripts lacking termination codons. *Science* **295**, 2258–2261 (2002).
9. Brandman, O. et al. A ribosome-bound quality control complex triggers degradation of nascent peptides and signals translation stress. *Cell* **151**, 1042–1054 (2012).
10. Shao, S., von der Malsburg, K. & Hegde, R. S. Listerin-dependent nascent protein ubiquitination relies on ribosome subunit dissociation. *Mol. Cell* **50**, 637–648 (2013).
11. Bengtson, M. H. & Joazeiro, C. A. P. Role of a ribosome-associated E3 ubiquitin ligase in protein quality control. *Nature* **467**, 470–473 (2010).
12. Pisareva, V. P., Skabkin, M. A., Hellen, C. U. T., Pestova, T. V. & Pisarev, A. V. Dissociation by Pelota, Hbs1 and ABCE1 of mammalian vacant 80S ribosomes and stalled elongation complexes. *EMBO J.* **30**, 1804–1817 (2011).
13. Shao, S., Brown, A., Santhanam, B. & Hegde, R. S. Structure and assembly pathway of the ribosome quality control complex. *Mol. Cell* **57**, 433–444 (2015).
14. Shen, P. S. et al. Rqc2p and 60S ribosomal subunits mediate mRNA-independent elongation of nascent chains. *Science* **347**, 75–78 (2015).
15. Lyumkis, D. et al. Structural basis for translational surveillance by the large ribosomalsubunit-associated protein quality control complex. *Proc. Natl Acad. Sci. USA* **111**, 15981–15986 (2014).
16. Verma, R., Oania, R. S., Kolawa, N. J. & Deshaies, R. J. Cdc48/p97 promotes degradation of aberrant nascent polypeptides bound to the ribosome. *eLife* **2**, e00308 (2013).
17. Defenouillère, Q. et al. Cdc48-associated complex bound to 60S particles is required for the clearance of aberrant translation products. *Proc. Natl Acad. Sci. USA* **110**, 5046–5051 (2013).
18. Defenouillère, Q. et al. Rqc1 and Ltn1 prevent C-terminal alanine-threonine tail (CAT-tail)-induced protein aggregation by efficient recruitment of Cdc48 on stalled 60S subunits. *J. Biol. Chem.* **291**, 12245–12253 (2016).
19. Osuna, B. A., Howard, C. J., Kc, S., Frost, A. & Weinberg, D. E. In vitro analysis of RQC activities provides insights into the mechanism and function of CAT tailing. *eLife* **6**, e27949 (2017).
20. Kuroha, K., Zinoviev, A., Hellen, C. U. T. & Pestova, T. V. Release of ubiquitinated and non-ubiquitinated nascent chains from stalled mammalian ribosomal complexes by ANKZF1 and Ptrh1. *Mol. Cell* **72**, 286–302.e8 (2018).
21. Kostova, K. K. et al. CAT-tailing as a fail-safe mechanism for efficient degradation of stalled nascent polypeptides. *Science* **357**, 414–417 (2017).
22. Izawa, T., Park, S.-H., Zhao, L., Hartl, F. U. & Neupert, W. Cytosolic protein Vms1 links ribosome quality control to mitochondrial and cellular homeostasis. *Cell* **171**, 890–903.e18 (2017).
23. Yonashiro, R. et al. The Rqc2/Tae2 subunit of the ribosome-associated quality control (RQC) complex marks ribosome-stalled nascent polypeptide chains for aggregation. *eLife* **5**, e11794 (2016).
24. Heo, J.-M. et al. A stress-responsive system for mitochondrial protein degradation. *Mol. Cell* **40**, 465–480 (2010).
25. Verma, R. et al. Vms1 and ANKZF1 peptidyl-tRNA hydrolases release nascent chains from stalled ribosomes. *Nature* **557**, 446–451 (2018).
26. Zurita Rendón, O. et al. Vms1p is a release factor for the ribosome-associated quality control complex. *Nat. Commun.* **9**, 2197 (2018).
27. Xiong, Y. & Steitz, T. A. A story with a good ending: tRNA 3′-end maturation by CCA-adding enzymes. *Curr. Opin. Struct. Biol.* **16**, 12–17 (2006).
28. Wilusz, J. E., Whipple, J. M., Phizicky, E. M. & Sharp, P. A. tRNAs marked with CCACCA are targeted for degradation. *Science* **334**, 817–821 (2011).
29. Shao, S. & Hegde, R. S. Reconstitution of a minimal ribosome-associated ubiquitination pathway with purified factors. *Mol. Cell* **55**, 880–890 (2014).
30. Klinge, S., Voigts-Hoffmann, F., Leibundgut, M., Arpagaus, S. & Ban, N. Crystal structure of the eukaryotic 60S ribosomal subunit in complex with initiation factor 6. *Science* **334**, 941–948 (2011).
31. Yang, W. Nucleases: diversity of structure, function and mechanism. *Q. Rev. Biophys.* **44**, 1–93 (2011).
32. Honda, S., Morichika, K. & Kirino, Y. Selective amplification and sequencing of cyclic phosphate-containing RNAs by the cP-RNA-seq method. *Nat. Protoc.* **11**, 476–489 (2016).
33. Schürer, H., Lang, K., Schuster, J. & Mörl, M. A universal method to produce in vitro transcripts with homogeneous 3′ ends. *Nucleic Acids Res.* **30**, e56 (2002).
34. Czech, A., Wende, S., Mörl, M., Pan, T. & Ignatova, Z. Reversible and rapid transfer-RNA deactivation as a mechanism of translational repression in stress. *PLoS Genet.* **9**, e1003767 (2013).
35. Zuo, Y. & Deutscher, M. P. The physiological role of RNase T can be explained by its unusual substrate specificity. *J. Biol. Chem.* **277**, 29654–29661 (2002).
36. Nagaike, T. et al. Identification and characterization of mammalian mitochondrial tRNA nucleotidyltransferases. *J. Biol. Chem.* **276**, 40041–40049 (2001).
37. Feng, Q. & Shao, S. In vitro reconstitution of translational arrest pathways. *Methods* **137**, 20–36 (2018).
38. Zinder, J. C. & Lima, C. D. Targeting RNA for processing or destruction by the eukaryotic RNA exosome and its cofactors. *Genes Dev.* **31**, 88–100 (2017).
39. Shigematsu, M., Kawamura, T. & Kirino, Y. Generation of 2′,3′-cyclic phosphate-containing RNAs as a hidden layer of the transcriptome. *Front. Genet.* **9**, 562 (2018).
40. Jilani, A. et al. Molecular cloning of the human gene, *PNKP*, encoding a polynucleotide kinase 3′-phosphatase and evidence for its role in repair of DNA strand breaks caused by oxidative damage. *J. Biol. Chem.* **274**, 24176–24186 (1999).
41. Karimi-Busheri, F. et al. Molecular characterization of a human DNA kinase. *J. Biol. Chem.* **274**, 24187–24194 (1999).
42. Mayer, M., Schiffer, S. & Marchfelder, A. tRNA 3′ processing in plants: nuclear and mitochondrial activities differ. *Biochemistry* **39**, 2096–2105 (2000).
43. Phizicky, E. M., Schwartz, R. C. & Abelson, J. *Saccharomyces cerevisiae* tRNA ligase. Purification of the protein and isolation of the structural gene. *J. Biol. Chem.* **261**, 2978–2986 (1986).
44. Popow, J. et al. HSPC117 is the essential subunit of a human tRNA splicing ligase complex. *Science* **331**, 760–764 (2011).
45. Phizicky, E. M. & Hopper, A. K. tRNA biology charges to the front. *Genes Dev.* **24**, 1832–1860 (2010).
46. Thompson, D. M., Lu, C., Green, P. J. & Parker, R. tRNA cleavage is a conserved response to oxidative stress in eukaryotes. *RNA* **14**, 2095–2103 (2008).
47. Fu, H. et al. Stress induces tRNA cleavage by angiogenin in mammalian cells. *FEBS Lett.* **583**, 437–442 (2009).
48. Yamasaki, S., Ivanov, P., Hu, G.-F. & Anderson, P. Angiogenin cleaves tRNA and promotes stress-induced translational repression. *J. Cell Biol.* **185**, 35–42 (2009).
49. Cole, S. E., LaRiviere, F. J., Merrikh, C. N. & Moore, M. J. A convergence of rRNA and mRNA quality control pathways revealed by mechanistic analysis of nonfunctional rRNA decay. *Mol. Cell* **34**, 440–450 (2009).

Acknowledgements

We thank A.E. Johnson, Y. Miao and Y. Shao for reagents and advice for producing tRNAs; J. Bridgers for help with the initial tRNA experiments; T. Guettler and D. Görlich for the SuperTEV expression plasmid; and R.S. Hegde, T.A. Rapoport, J.W. Harper, A. Brown, S. Juszkiewicz and Shao Laboratory members for useful discussions. This work was supported by Harvard Medical School startup funds, a Richard and Susan Smith Family Award for Excellence in Biomedical Research, a Charles H. Hood Foundation Child Health Research Award, and the Vallee Scholars Program (to S.S.), a NDSEG predoctoral fellowship (V.C.), the Jane Coffin Childs Memorial Fund for Medical Research (61-1681 to Q.F.), and an American Heart Association postdoctoral fellowship (19POST34400009 to M.J.M.).

Author contributions

M.C.J.Y. and S.S. designed, performed and analyzed the experiments with help from A.F.A.K, Q.F., V.C. and M.J.M. S.S. wrote the manuscript with input from all authors.

Competing interests

The authors declare no competing interests.

Additional information

Supplementary information is available for this paper at https://doi.org/10.1038/s41594-019-0211-4.

Reprints and permissions information is available at www.nature.com/reprints.

Correspondence and requests for materials should be addressed to S.S.

Publisher's note: Springer Nature remains neutral with regard to jurisdictional claims in published maps and institutional affiliations.

Methods

Plasmids and antibodies. All constructs used for coupled in vitro transcription and translation were in an SP64 vector[37]. Truncated templates encoding Flag-tagged villin head piece-beta constructs (Figs. 1a and 2a) were prepared exactly as in our previous studies[10,13,29] by PCR amplification using a forward primer that anneals slightly upstream of the SP6 promoter and a reverse primer defining the 3′ mRNA truncation point. The open reading frames of Pelota, eIF6, wild-type and mutant Vms1p proteins, TRNT1 and human eRF1 were subcloned into the pRSETA expression vector encoding a C-terminal His tag. Pelota, eIF6 and eRF1 constructs were described previously[29,50]. Vms1p was subcloned from yeast genomic DNA; TRNT1 (HsCD00329081) complementary DNA was obtained from the PlasmID Repository at Harvard Medical School. Wild-type and dominant negative Hbs1L, ABCE1, NEMF and Listerin in a pcDNA3.1 mammalian expression vector were described previously[13,29]. The wild-type ANKZF1 cDNA sequence (HsCD00322220) obtained from the PlasmID Repository was subcloned into a pcDNA3.1-based expression vector. Point mutations were made using Phusion High-Fidelity DNA polymerase (New England Biolabs) mutagenesis according to the manufacturer's instructions.

In vitro transcription templates of $tRNA^{Leu}$ were prepared by amplifying ultramers or a plasmid encoding the tRNA sequence using primer pairs encoding a T7 promoter and the desired 3′ sequence, as shown in Table 1. The HDV ribozyme deletion variant[33] was added to the 3′ end of the appropriate $tRNA^{Leu}$ constructs in a plasmid using blunt-end ligation.

Antibodies against TRNT1 (catalog no. NBP1-86589; Novus Biologicals), PNKP (catalog no. NBP1-87257; Novus Biologicals), aprataxin and PNK-like factor (catalog no. 14252-1-AP; Proteintech), ANKZF1 (catalog no. sc-398713; Santa Cruz Biotechnology) and mitochondrial import receptor subunit TOM20 homolog (catalog no. sc-17764; Santa Cruz Biotechnology) were purchased. Small interfering RNAs against TRNT1 (L-015850-00-0005) and PNKP (L-006783-00-0005) were obtained from Dharmacon.

Recombinant proteins. Pelota, eIF6, eRF1, wild-type and mutant Vms1p proteins were expressed and purified in BL21(DE3) or Rosetta 2 competent cells using standard procedures. Briefly, competent cells were transformed with the appropriate pRSETA vector, grown to an absorbance A_{600} of 0.6–0.8 in lysogeny broth under antibiotic selection, and induced with 0.2 mM isopropyl-β-D-thiogalactopyranoside overnight at 16 °C. Cells were collected via centrifugation and resuspended in lysis buffer (1× PBS, 250 mM NaCl, 10 mM imidazole, 1 mM dithiothreitol (DTT) and protease inhibitor cocktail) and lysed by two passages through a microfluidizer. Lysates were cleared via centrifugation and the supernatant passed over pre-equilibrated Ni-NTA resin. The resin was washed with 10 column volumes of lysis buffer, and eluted in 1× PBS, 250 mM NaCl, 200 mM imidazole and 1 mM DTT. Peak elutions were pooled and dialyzed into dialysis buffer (25 mM HEPES, pH 7.5, 150 mM KOAc, 5 mM $Mg(OAc)_2$, 10 mM imidazole, 10% glycerol and 1 mM DTT) overnight in the presence of 1:100 w/w Tobacco Etch Virus protease. The cleaved His tag and Tobacco Etch Virus protease were subtracted after dialysis over a nickel column. Purified proteins were pooled, concentrated and stored in aliquots for subsequent use.

Wild-type and dominant negative Hbs1L, ABCE1, NEMF and ANKZF1 were expressed and purified from HEK293T cells as described previously[29]. Briefly, a 10 cm plate of 60–70% confluent HEK293T cells was transfected with 7 µg of the expression plasmid using *Trans*IT-293 transfection reagent (Mirus Bio) according to the manufacturer's protocols and split 1:4 the next day. Seventy-two hours after transfection, cells were collected in cold PBS and lysed in lysis buffer (50 mM HEPES, pH 7.5, 100 mM KOAc, 5 mM $Mg(OAc)_2$, 1 mM DTT and 0.5% Triton X-100). After clarification by centrifugation, lysates were incubated with ANTI-FLAG M2 resin (Sigma-Aldrich) for 1 h at 4 °C and washed sequentially with lysis buffer, wash buffer (50 mM HEPES, pH 7.5, 400 mM KOAc, 5 mM $Mg(OAc)_2$, 1 mM DTT and 0.5% Triton X-100) and RNC buffer (50 mm HEPES, 100 mM KOAc, 5 mM $Mg(OAc)_2$ and 1 mM DTT). Elutions were carried out with 0.15 mg ml^{-1} 3X Flag Peptide (Sigma-Aldrich) in RNC buffer at room temperature for 20–30 min.

tRNA production. tRNAs were transcribed using T7 RNA polymerase. Transcription templates (2–4 ng $µl^{-1}$) containing the T7 promoter and tRNA sequence were amplified using PCR and added to transcription reactions containing 60 mM HEPES (pH 7.5), 25 mM NaCl, 18 mM $MgCl_2$, 2 mM spermidine, 10 mM DTT, 0.5 mM nucleoside triphosphate (NTP) and 0.2 U $µl^{-1}$ recombinant RNasin ribonuclease inhibitors (Promega) in a total volume of 60 µl. For radiolabeling, [α-^{33}P]-CTP or [α-^{33}P]-UTP (PerkinElmer) were added at a 1:1 ratio to the corresponding unlabeled nucleotide (0.25 mM each). Reactions were incubated at 37 °C for 4 h and stopped with the addition of 1 volume of TRIzol and 0.2 volumes of chloroform. The aqueous phase was ethanol-precipitated overnight at −20 °C and resuspended in 50 µl of water.

In vitro translations, affinity purifications and reconstituted reactions. Coupled in vitro transcription and translation reactions were performed as described in a home-made RRL translation system[37]. Templates for translation were transcribed in reactions containing 76% v/v transcription mix, 0.4 U $µl^{-1}$ RNasin, 0.2 U $µl^{-1}$SP6 RNA polymerase (New England Biolabs) and 2.5 ng $µl^{-1}$ template (amplified by PCR). The reactions were incubated at 37 °C for 1 h. The products of the transcription reaction (5% final volume) were directly added to translation reactions containing 50% v/v cT2 mix (with or without supplementation with liver tRNAs), 0.04 mM methionine and, where applicable, 16 ng $µl^{-1}$ of in vitro transcribed $tRNA^{Leu}$. Depending on the reactions, either the methionine or tRNA was radiolabeled. Translation reactions were carried out at 32 °C for 30 min.

To purify RNCs (Figs. 1 and 2)[13,29], 50 nM of dominant negative Hbs1 was added 7 min after the translation reactions were initiated. Translation reactions were allowed to proceed for a total of 25–30 min, adjusted to 750 mM KOAc and 15 mM $Mg(OAc)_2$, and centrifuged over a 0.5 M sucrose cushion in 50 mM HEPES, pH 7.5, 750 mM KOAc and 5 mM $Mg(OAc)_2$ in a TLA-100.3 fixed-angle rotor (Beckman Coulter) at 100,000 r.p.m. for 1 h at 4 °C. Ribosomal pellets were resuspended in RNC buffer, incubated with M2 resin for 1 h at 4 °C, washed sequentially with RNC buffer + 0.1% Triton X-100, wash buffer (50 mM HEPES, pH 7.5, 250 mM KOAc, 5 mM $Mg(OAc)_2$, 1 mM DTT and 0.5% Triton X-100) and RNC buffer. Elutions were carried out with 0.15 mg ml^{-1} 3X Flag Peptide in RNC buffer at room temperature for 20–30 min. Elutions were directly used or further concentrated by centrifugation in a TLA-120.2 fixed-angle rotor (Beckman Coulter) at 100,000 r.p.m. for 40 min. For reconstituted reactions, RNCs were incubated with an energy-regenerating system (1 mM ATP, 1 mM GTP, 20 µg ml^{-1} creatine kinase and 12 mM creatine phosphate) and recombinant proteins. Unless otherwise indicated, concentrations were as follows: 5–10 nM RNCs (estimated based on non-radiolabeled preparations); 50 nM Hbs1L; 50 nM Pelota; 100 nM ABCE1; 10 nM NEMF; 5–10 nM Listerin; 75 nM E1 enzyme (Boston Biochem); 250 nM ubiquitin-conjugating Enzyme H5a (Boston Biochem); 10 µM His- or HA-tagged ubiquitin (Boston Biochem); 12.5 nM or 25 nM ANKZF1; and 25 nM or 125 nM Vms1p. Reactions were carried out at 32 °C for 15 min unless otherwise stated. Reactions with ubiquitin-specific-processing protease 2 (USP2) catalytic domain (Boston Biochem; Fig. 1c) were carried out for 15 min at 32 °C.

RNA reactions. T4 PNK (New England Biolabs) treatments (Fig. 3) were performed on RNAs in either 100 mM Tris (pH 6.5), 100 mM $Mg(OAc)_2$, 5 mM β-mercaptoethanol or PSB (50 mM HEPES, pH 7.5, 100 mM KOAc, 2.5 mM $Mg(OAc)_2$ and 1 mM DTT) with 6 U of T4 PNK in a reaction volume of 50 µl at 37 °C for 30 min to 6 h. Exonuclease T (New England Biolabs) reactions (Figs. 2d and 4d and Supplementary Fig. 7a) were performed in Buffer 4 (New England Biolabs) at 25 °C for 30 min. Calf intestinal phosphatase (CIP; New England Biolabs) reactions (Fig. 4c) were performed in CutSmart Buffer (New England Biolabs) with 10 U of CIP in a reaction volume of 50 µl at 37 °C for 30 min. TRNT1 reactions (Figs. 3 and 4) were performed on RNAs in PSB with 100 nM recombinant

Table 1 | In vitro transcription templates of $tRNA^{Leu}$

LeuTAA tRNA	ACCAGGATGGCCGAGTGGTTAAGGCGTTGGACTTAAGATCCAATGGACATATGTCCGCGTGGGTTCGAACCCCACTCCTGGTACCA
LeuTAA_T7_F	AAGGGAATTCTAATACGACTCACTATTACCAGGATGGCCGAGTGGTTAAGG
LeuTAA_FL_R	TGGTACCAGGAGTGGGGTTCG
LeuTAA_CCA_R	TACCAGGAGTGGGGTTCGAAC
LeuTAA_ACCA_R	ACCAGGAGTGGGGTTCGAACC
LeuTAA_CA_R	GTACCAGGAGTGGGGTTCGAAC
LeuTAA_A_R	GGTACCAGGAGTGGGGTTCG
LeuCAG tRNA	GTCAGGATGGCCGAGCGGTCTAAGGCGCTGCGTTCAGGTCGCAGTCTCCCCTGGAGGCGTGGGTTCGAATCCCACTCCTGACACCA
LeuCAG_T7_F	AAGGGAATTCTAATACGACTCACTATAGTCAGGATGGCCGAGCGGTCTAAGG
LeuCAG_FL_R	TGGTGTCAGGAGTGGGATTCGAACC
HDV	GGGTCGGCATGGCATCTCCACCTCCTCGCGGTCCGACCTGGGCTACTTCGGTAGGCTAAGGGAGAAG

TRNT1 and 0.5 mM NTPs at 37 °C for 30 min. Reactions containing both T4 PNK and TRNT1 (Fig. 3e) were performed in PSB and incubated at 32 °C for 30 min. Reactions with RRL or cytosolic lysate isolated from HEK293 or HEK293T cells (Fig. 4c–e) were performed with 50% v/v RRL or 6.7 mg ml^{-1} hypotonic lysate in PSB with 0.5 mM NTPs, 10 µg ml^{-1} creatine kinase, 6 mM creatine phosphate and 2% v/v RNase inhibitor (Promega) at 32 °C for 30 min. All reactions were stopped by adding TRIzol. RNAs were subject to TRIzol-chloroform extraction and ethanol precipitation, or isolated via Direct-zol columns (Zymo Research).

Cell culture and lysate generation. HEK293 and HEK293T cell lines were originally obtained from ATCC. They were verified by short tandem repeat profiling and are checked yearly to verify that they are free of *Mycoplasma* contamination. To generate hypotonic lysates, HEK293 or HEK293T cells were collected and pelleted in cold PBS. Cells were resuspended in an equal cell pellet volume of hypotonic buffer (10 mM HEPES, pH 7.5, 10 mM KOAc, 1.5 mM $Mg(OAc)_2$ and 1 mM DTT). After 30 min on ice, cells were lysed through a 26 G needle and clarified by centrifugation. The supernatant was used directly for subsequent reactions. Where applicable, knockdowns (Fig. 4e and Supplementary Fig. 8i) were performed on 10 cm plates of 50–60% confluent HEK293T cells for 72 h using 145 pmol siRNA (Dharmacon) and Lipofectamine RNAiMAX Transfection Reagent (Thermo Fisher Scientific) according to the manufacturer's instructions. All mammalian cells were cultured in DMEM (high glucose; GlutaMAX supplement; Thermo Fisher Scientific) with 10% fetal bovine serum at 37 °C and 5% CO_2.

Miscellaneous biochemistry. Denaturing immunoprecipitations were performed by adding an equal volume of 100 mM Tris (pH 6.5) and 2% SDS to translation reactions and boiled at 98 °C for 1.5 min. Reactions were incubated with 1 ml of cold immunoprecipitation buffer (1× RNC buffer + 1% Triton X-100) and 10 µl of pre-equilibrated Flag resin at 4 °C for 1 h. The resin was washed three times with 1 ml applications of cold immunoprecipitation buffer and eluted by boiling in 25 µl of protein sample buffer. SDS–polyacrylamide gel electrophoresis (PAGE), NuPAGE, and 10% and 15% Tris/Borate/EDTA (TBE)–urea–PAGE gels were cast using Bio-Rad Laboratories plates and stands using standard procedures.

Reporting Summary. Further information on research design is available in the Nature Research Reporting Summary linked to this article.

Data availability

All data generated or analyzed during this study are included in this published article and its Supplementary information files.

References

50. Brown, A., Shao, S., Murray, J., Hegde, R. S. & Ramakrishnan, V. Structural basis for stop codon recognition in eukaryotes. *Nature* **524**, 493–496 (2015).

nature structural & molecular biology

SUPPLEMENTARY INFORMATION

https://doi.org/10.1038/s41594-019-0211-4

In the format provided by the authors and unedited.

Mechanism for recycling tRNAs on stalled ribosomes

Matthew C. J. Yip, Alexander F. A. Keszei, Qing Feng, Vincent Chu, Michael J. McKenna and Sichen Shao*

Department of Cell Biology, Harvard Medical School, Boston, MA, USA. *e-mail: sichen_shao@hms.harvard.edu

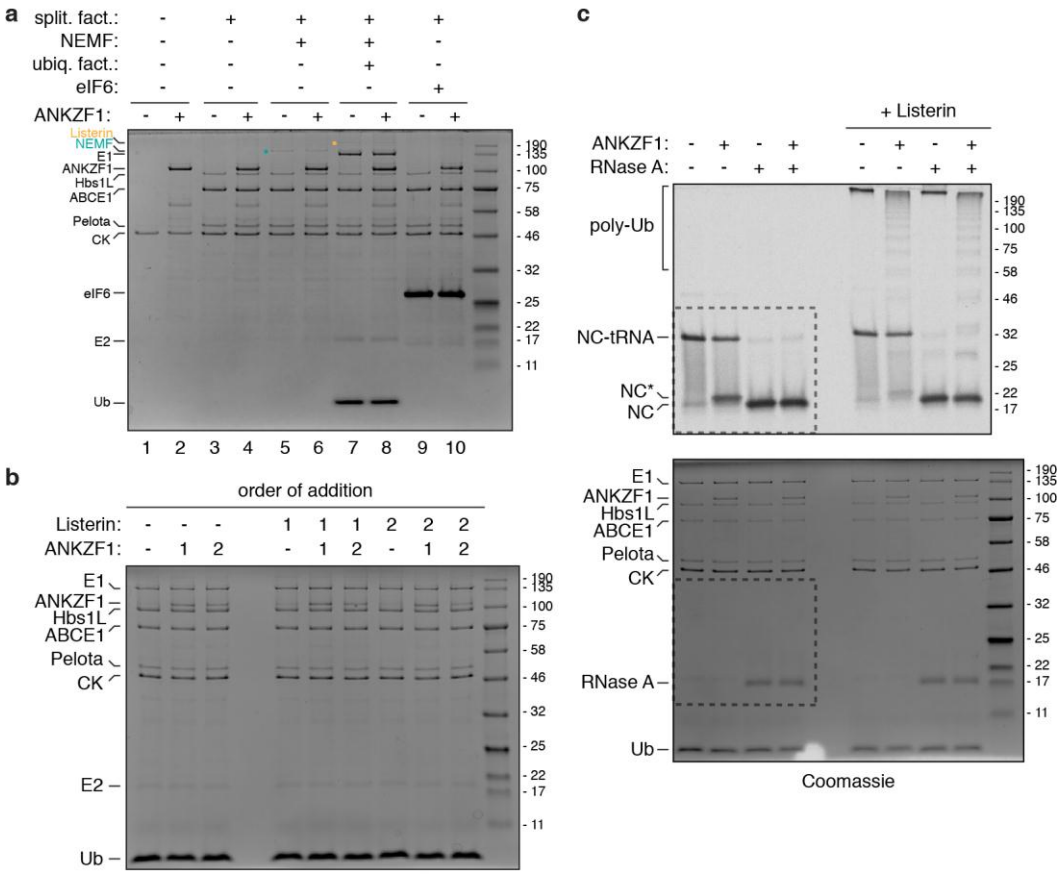

Supplementary Figure 1

Reconstitution of ANKZF1 activity with purified factors.

Coomassie stain of the SDS-PAGE gel analyzed by autoradiography in **a,** Fig. 1b and **b,** Fig. 1c. Individual recombinant proteins are indicated. **c,** Full-sized autoradiography (top) and Coomassie stained (bottom) SDS-PAGE gel in Fig. 1d, with cropped area indicated, demonstrating the effect of RNase A on Listerin-ubiquitinated substrates treated without or with ANKZF1. split. fact. – ribosome splitting factors (50 nM Hbs1L, 50 nM Pelota, 100 nM ABCE1); ubiq. fact. – ubiquitination factors (75 nM E1, 250 nM E2, 5 nM Listerin, 10 μM ubiquitin); CK – creatine kinase, part of an energy regenerating system; Ub – ubiquitin; NC-tRNA – nascent chain-tRNA; NC* - ANKZF1-cleaved nascent chain; NC – nascent chain; poly-Ub – poly-ubiquitinated nascent chain.

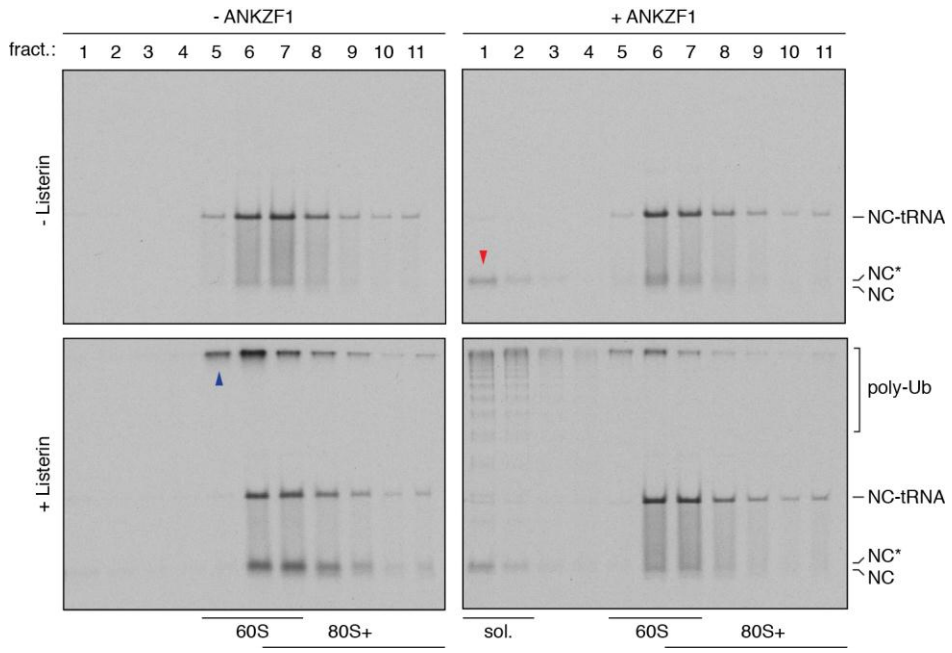

Supplementary Figure 2

ANKZF1 releases nascent proteins from ribosomes.

5 nM of purified 80S ribosome-nascent protein complexes (RNCs, as in Fig. 1a) containing radiolabeled nascent protein were incubated with an energy regenerating system, ribosome splitting factors (50 nM Hbs1L, 50 nM Pelota, 100 nM ABCE1), 10 nM NEMF, 75 nM E1, 250 nM E2, 10 μM ubiquitin, and the indicated combinations of 5 nM Listerin and/or 25 nM ANKZF1. 20 μL reactions were size fractionated on 200 μL 10-50% sucrose gradients. Eleven 20 μL fractions (fract.) collected from the top of the gradients were analyzed directly by SDS-PAGE and autoradiography. Migration of radiolabeled nascent polypeptide chain (NC), nascent chain-tRNA (NC-tRNA), ANKZF1-cleavage product (NC*; red arrow) and ubiquitinated nascent proteins (poly-Ub) are indicated. In the absence of ANKZF1, Listerin-mediated ubiquitination occurs on 60S ribosomal subunits (blue arrow), while ANKZF1-cleaved products are released from ribosomal to soluble (sol.) fractions (right gels).

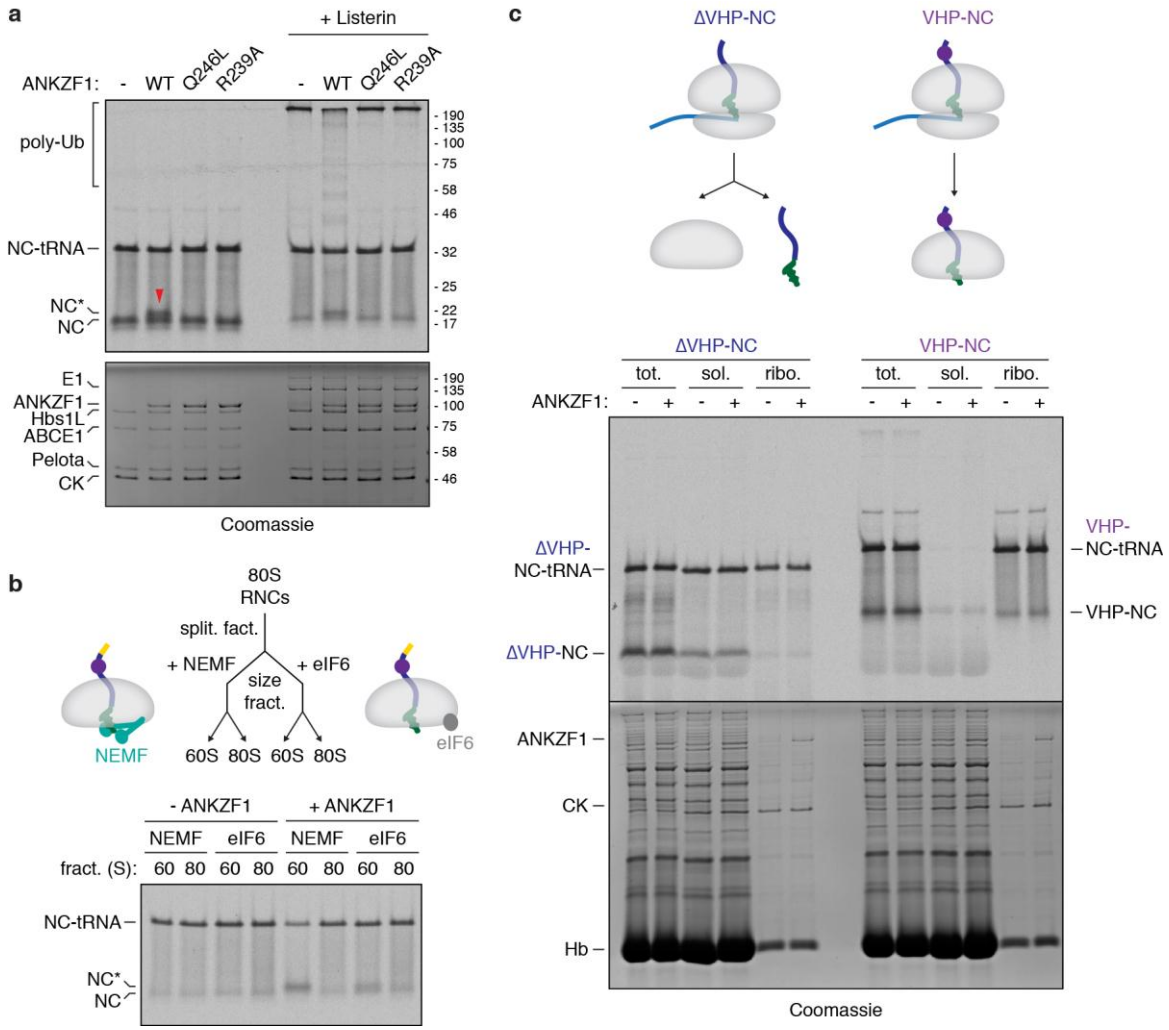

Supplementary Figure 3

ANKZF1 selectively acts on 60S RQC complexes.

a, 5 nM 80S RNCs were incubated with energy, 50-100 nM splitting factors, 10 nM NEMF, 12.5 nM wildtype (WT) or the indicated ANKZF1 mutants without (left) or with (right) ubiquitination reagents. Reactions were analyzed by SDS-PAGE and autoradiography (top), and a portion of the Coomassie stained gel is shown (bottom). This demonstrates that mutations in the putative catalytic loop of ANKZF1 abolishes nascent protein release (red arrow). **b,** 80S RNCs were incubated with energy, splitting factors, and either NEMF or eIF6. Schemes of how NEMF and eIF6 prevent 40S rejoining are shown. 200 μL of these splitting reactions were separated by size into 25 fractions on a 4.8 mL 10-30% sucrose gradient. Fractions containing 60S or 80S ribosomal subunits were pooled and incubated without (left) or with (right) 25 nM ANKZF1. Note that only nascent polypeptidyl-tRNA on 60S ribosomal subunits, but not 80S ribosomes, are cleaved by ANKZF1. eIF6, which does not bind directly to peptidyl-tRNA at the 60S ribosomal subunit interface as NEMF does, is less effective at mediating ANKZF1 activity. **c,** Cell-free translation reactions of model substrates without (ΔVHP) or with the autonomously folding villin-headpiece domain (VHP) were separated on a 10-50% sucrose gradient. Short nascent proteins without folded domains 'slip out' of ribosomes upon splitting. Soluble (fractions 1-3) and ribosomal (fractions 5-8) fractions were pooled and incubated with 25 nM ANZKF1. Reactions were analyzed by SDS-PAGE and autoradiography (top) and Coomassie staining (bottom) This demonstrates that ANKZF1 does not act on soluble NC-tRNA or ribosome-associated NC-tRNA in the absence of ribosome splitting.

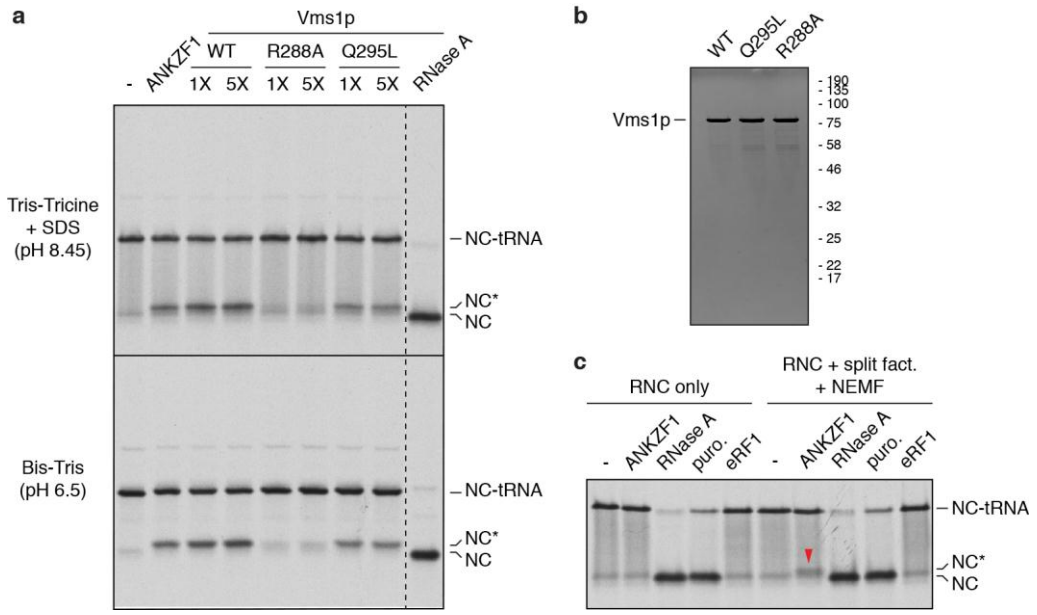

Supplementary Figure 4

ANKZF1 and Vms1p cleave peptidyl-tRNA.

a, 5 nM RNCs were incubated with energy, 50-100 nM splitting factors, 10 nM NEMF, and 25 nM ANKZF1 or 25 nM (1X) or 125 nM (5X) of wildtype (WT) or mutant Vms1p, the yeast homolog of ANKZF1. Reactions were analyzed by SDS-PAGE (top) or NuPAGE (bottom) and autoradiography. Note that yeast Vms1p generates the same cleavage product as ANKZF1 and also relies on conserved residues in the catalytic loop. In addition, the lower pH of NuPAGE gels better preserves peptidyl-tRNA bonds which are susceptible to hydrolysis in basic Tris-tricine gels. Thus, for experiments to analyze ANKZF1- and Vms1p-generated products (Fig. 2-4), we switched primarily to NuPAGE to facilitate detection of tRNA-associated products, and to using 125 nM Vms1p, which we were able to obtain at higher concentrations and purities than ANKZF1, to optimize cleavage efficiency. **b,** Coomassie stain of purified Vms1p proteins. **c,** 5 nM purified 80S RNCs were incubated with the indicated components (12.5 nM ANKZF1, 50 μg/mL RNase A, 1 mM puromycin, 1 μM eRF1). Red arrow depicts ANKZF1 cleavage product (NC*), which requires ribosome splitting and NEMF. NC* is larger than the expected size of nascent chain (NC) produced by RNase A or puromycin (puro.) treatment. NC-tRNA – nascent polypeptidyl-tRNA, eRF1 – eukaryotic release factor 1. Note that the translation termination factor eRF1 is not expected to act catalytically on these substrates due to the lack of a stop codon.

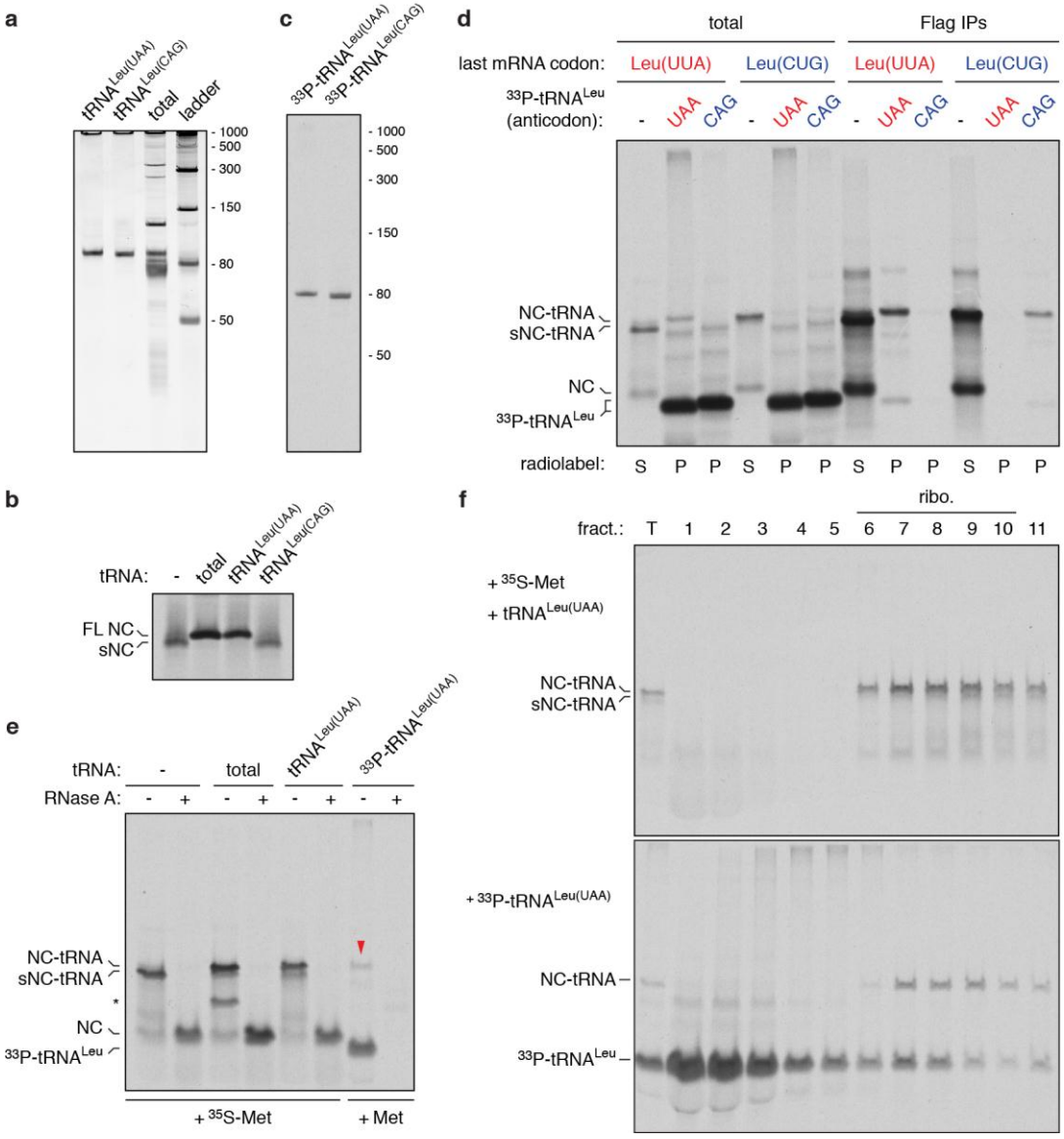

Supplementary Figure 5

tRNA^{Leu} selectively incorporates into ribosome-nascent protein complexes.

a, TBE-urea-PAGE and SYBR Gold comparison of transcribed leucyl-tRNA (tRNA^{Leu}) containing either the UAA (tRNA$^{Leu(UAA)}$) or the CAG (tRNA$^{Leu(CAG)}$) anticodon, and total mammalian liver tRNAs. **b,** Cell-free translation reactions of radiolabeled protein containing three consecutive rare leucine UUA codons[37] without or with total mammalian liver tRNAs or leucyl-tRNAs with the indicated anticodon. Translation stalls at the rare leucine codons, generating a truncated nascent chain (sNC), unless reactions are supplemented with leucyl-tRNA with the cognate UAA codon (which is also present in total liver tRNAs) to rescue translation of the full-length nascent chain (FL NC). Note that tRNA$^{Leu(UAA)}$, but not tRNA$^{Leu(CAG)}$, rescues translation of FL NC. **c,** The indicated radiolabeled tRNAs were transcribed and analyzed by TBE-urea-PAGE and autoradiography. **d,** Truncated mRNAs ending in the indicated leucine codon (UUA or CUG) were translated without additional tRNA in the presence of ^{35}S-methionine (S), or in the presence of ^{33}P-radiolabeled leucyl-tRNA (P) with the indicated anticodon. Reactions were directly analyzed by NuPAGE and autoradiography (left) or first subjected to denaturing immunoprecipitations against an N-terminal Flag epitope tag (Flag IPs) encoded in the nascent protein sequence (right). This demonstrates that radiolabeled leucyl-tRNA specifically incorporates into ribosome-nascent protein complexes (RNCs) stalled at the cognate codon. **e,** Cell-free translation reactions of a truncated mRNA ending in two consecutive rare UAA codons (as in Fig. 2a) in an endogenous rabbit reticulocyte translation system supplemented

with no additional tRNA, 0.2 mg/mL pig liver tRNAs, or 0.5% (v/v) of nonradiolabeled or ^{33}P-labeled tRNA^{Leu}. Reactions lacking radiolabeled tRNA^{Leu} contained ^{35}S-methionine to radiolabel the nascent protein. Reactions were directly analyzed before or after RNase A treatment by NuPAGE and autoradiography to compare labeling efficiencies of the nascent chain-tRNA (NC-tRNA, red arrow). sNC-tRNA refers to the stalled products on the rare UAA codons in the absence of tRNA supplementation. **f,** Cell-free translation reactions as in **a** containing ^{35}S-methionine and nonradiolabeled tRNA^{Leu} (top) or cold methionine and radiolabeled tRNA^{Leu} (bottom) were separated on a 10-50% sucrose gradient. Eleven fractions were collected from the top and analyzed by NuPAGE and autoradiography. This demonstrates that radiolabeled NC-tRNA products are ribosome-associated, while free tRNA remains soluble.

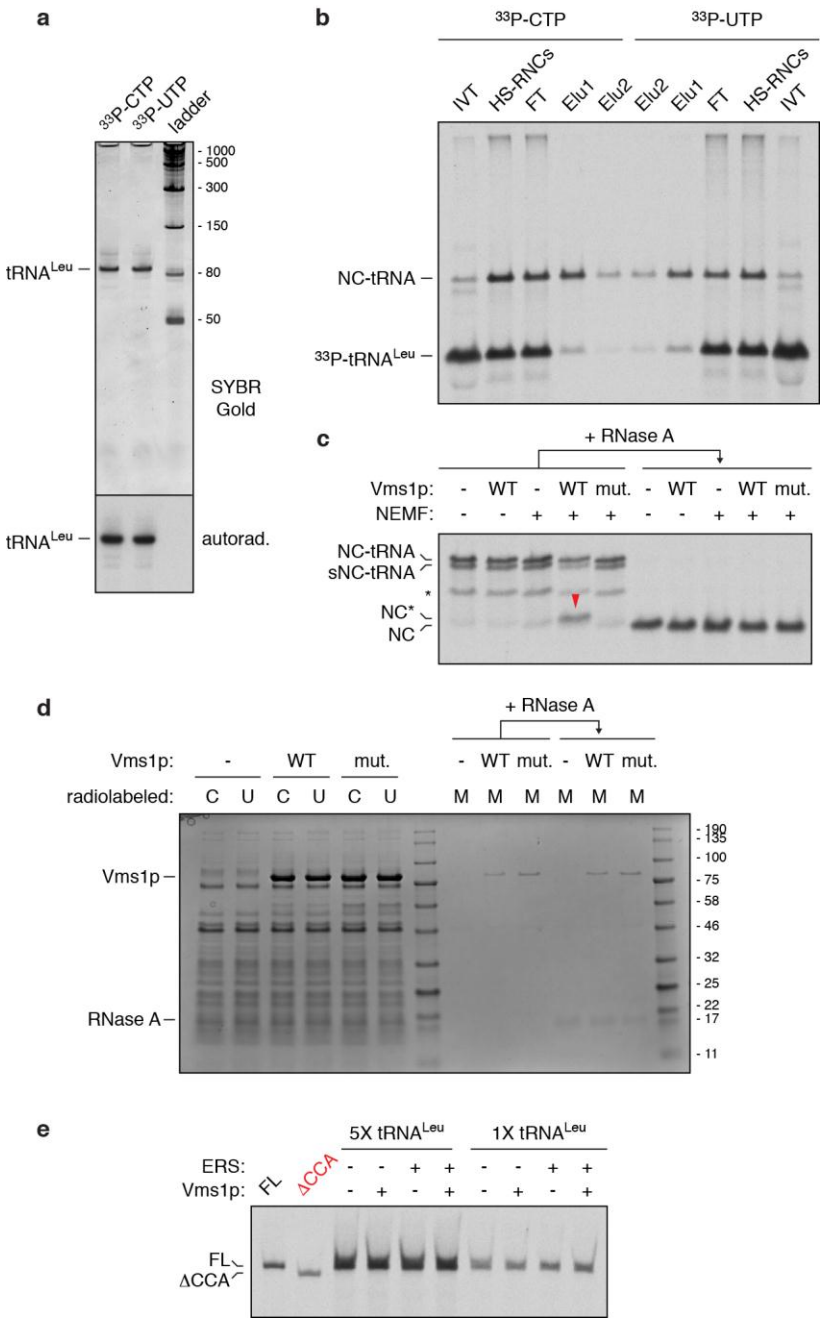

Supplementary Figure 6

Isolation and Vms1p cleavage of RNCs with radiolabeled peptidyl-tRNA^{Leu}.

a, TBE-urea-PAGE and SYBR Gold (top) or autoradiography (bottom) analysis of tRNA^{Leu} transcribed with either radiolabeled CTP or UTP. **b,** Purification of stalled 80S ribosome-nascent chain complexes (RNCs) from cell-free translation reactions of the truncated mRNA depicted in Fig. 2a with either C- or U-labeled tRNA^{Leu}. IVT – total in vitro translation reaction; HS-RNCs – high-salt-washed RNCs; FT – flow-through; Elu – elution. **c,** ^{35}S-methionine labeled RNCs generated using the same model mRNA as in **b** with total liver tRNAs were incubated with energy, 50-100 nM ribosome splitting factors, and 10 nM NEMF and 125 nM wildtype (WT) or R288A (mut.) Vms1p as indicated. Reactions were directly analyzed before or after RNase A treatment by NuPAGE and autoradiography. This demonstrates that the requirements for Vms1p activity on RNCs containing peptidyl-tRNA^{Leu} are identical to

those containing peptidyl-$tRNA^{Val}$ (Fig. 1). **d,** Coomassie stain of the SDS-PAGE gel analyzed in Fig. 2b. Note that 20-fold less of the reactions containing ^{35}S-methionine-labeled RNCs were loaded to roughly normalize the autoradiography signals. **e,** Radiolabeled $tRNA^{Leu}$ at approximately one (1X) or five (5X) times the concentration isolated from RNCs (e.g. Fig. 2c) was incubated with 125 nM Vms1p without or with an energy regenerating system (ERS). Without being incorporated into RNCs, there is no noticeable Vms1p cleavage of free tRNAs. Transcribed $tRNA^{Leu}$ with (FL) or without (ΔCCA) the 3'CCA nucleotides are loaded as size markers.

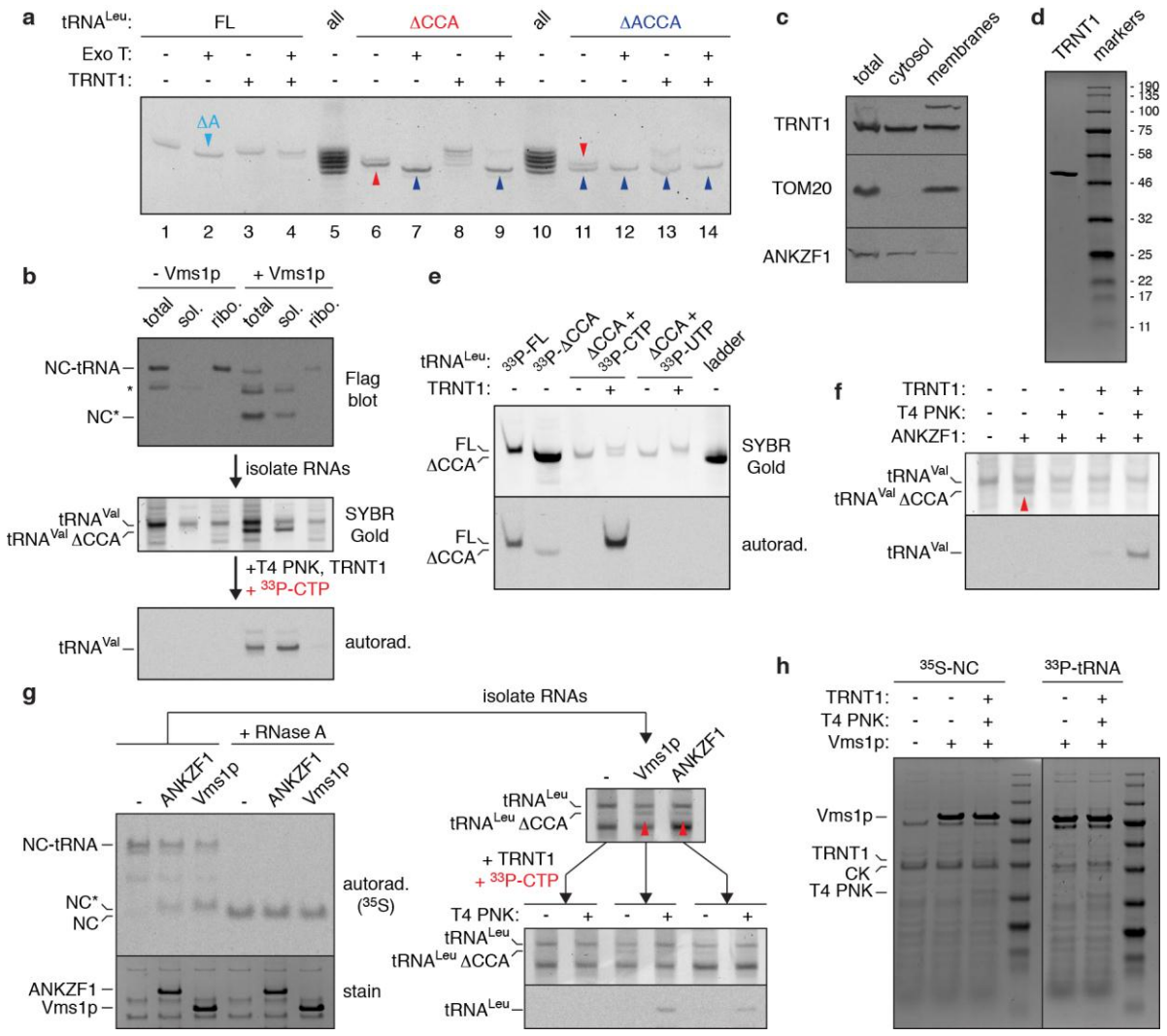

Supplementary Figure 7

Reconstitution of TRNT1-mediated tRNA recycling.

a, Full-length (FL) $tRNA^{Leu}$ or $tRNA^{Leu}$ lacking three (ΔCCA, red) or four (ΔACCA, dark blue) 3' terminal nucleotides were transcribed *in vitro* and treated with 0.05 U/μL Exonuclease T (Exo T), followed by 100 nM recombinant TRNT1 as indicated. Reactions were analyzed by TBE-urea-PAGE and SYBR Gold staining. Note that Exonuclease T removes a single nucleotide from FL (lane 2, light blue arrow) and ΔCCA $tRNA^{Leu}$ (lane 7, dark blue arrow), consistent with its activity as a single-stranded 3' to 5' exonuclease that is inhibited by consecutive cytidine nucleotides. The two C nucleotides of the 3'CCA prevent further digestion of FL $tRNA^{Leu}$, while basepairing (Fig. 2a) prevents further digestion of ΔCCA $tRNA^{Leu}$. TRNT1 repairs tRNAs lacking one (compare lanes 2 and 4) or three (compare lanes 6 and 8) 3' nucleotides, but not those lacking four (lanes 9, 13, and 14, dark blue arrows). The slight repair seen in lane 13 is from the small amount of product lacking three 3' terminal nucleotides (red arrow, lane 11) generated by heterogeneous transcription of the ΔACCA $tRNA^{Leu}$ construct without Exonuclease T digestion. **b,** Vms1p cleavage reactions (total) of non-radiolabeled RNCs ending in valyl-tRNA ($tRNA^{Val}$) as in Supplementary Fig. 4a were separated on a 10-50% sucrose gradient. Soluble (sol.) and ribosomal (ribo.) fractions were pooled and analyzed by immunoblotting against the Flag-tagged nascent protein (top) or subjected to RNA extraction, TBE-urea-PAGE, and SYBR Gold staining (middle). The extracted RNAs were also used in TRNT1 repair reactions (as in Fig. 3b) with T4 PNK and radiolabeled CTP, and analyzed by TBE-urea-PAGE and autoradiography (bottom). Note that the tRNA fragment generated by Vms1p is exclusively in the soluble fraction, indicating that it is released from RNCs after cleavage. **c,** HEK293T cells were harvested (total) and sequentially fractionated with 100 μg/mL digitonin to isolate cytosol and 1% Triton X-100 to solubilize organellar membranes. Individual fractions were analyzed by SDS-PAGE and

immunoblotting for the indicated components. TOM20 is a mitochondrial outer membrane protein. **d,** Coomassie stain of purified TRNT1 lacking the N-terminal mitochondrial transit peptide. **e,** The indicated nonradiolabeled transcribed $tRNA^{Leu}$ constructs were incubated with TRNT1 in the presence of radiolabeled CTP or UTP. This demonstrates that cytidine is specifically incorporated into TRNT1-repaired products. **f,** Non-radiolabeled RNCs ending in $tRNA^{Val}$ were subjected to cleavage and TRNT1 repair reactions exactly as in Fig. 3c, except with mammalian ANKZF1 instead of yeast Vms1p. **g,** Side-by-side cleavage reactions of ^{35}S-radiolabeled RNCs ending in leucyl-tRNA ($tRNA^{Leu}$) with mammalian ANKZF1 or yeast Vms1p, demonstrating that both generate the identical NC* product sensitive to RNase A (left). RNAs were extracted from these reactions (right) and analyzed directly (top) or subject to TRNT1 repair reactions in the presence of radiolabeled CTP with or without T4 PNK (bottom). Note that the Vms1p and ANKZF1 lanes are switched between the protein (left) and RNA (right) gels, but that both generate the same tRNA fragment that is selectively repaired by TRNT1 only after the removal of the 2',3'-cyclic phosphate by T4 PNK. **h,** Coomassie stain of SDS-PAGE gels analyzed in Fig. 3e.

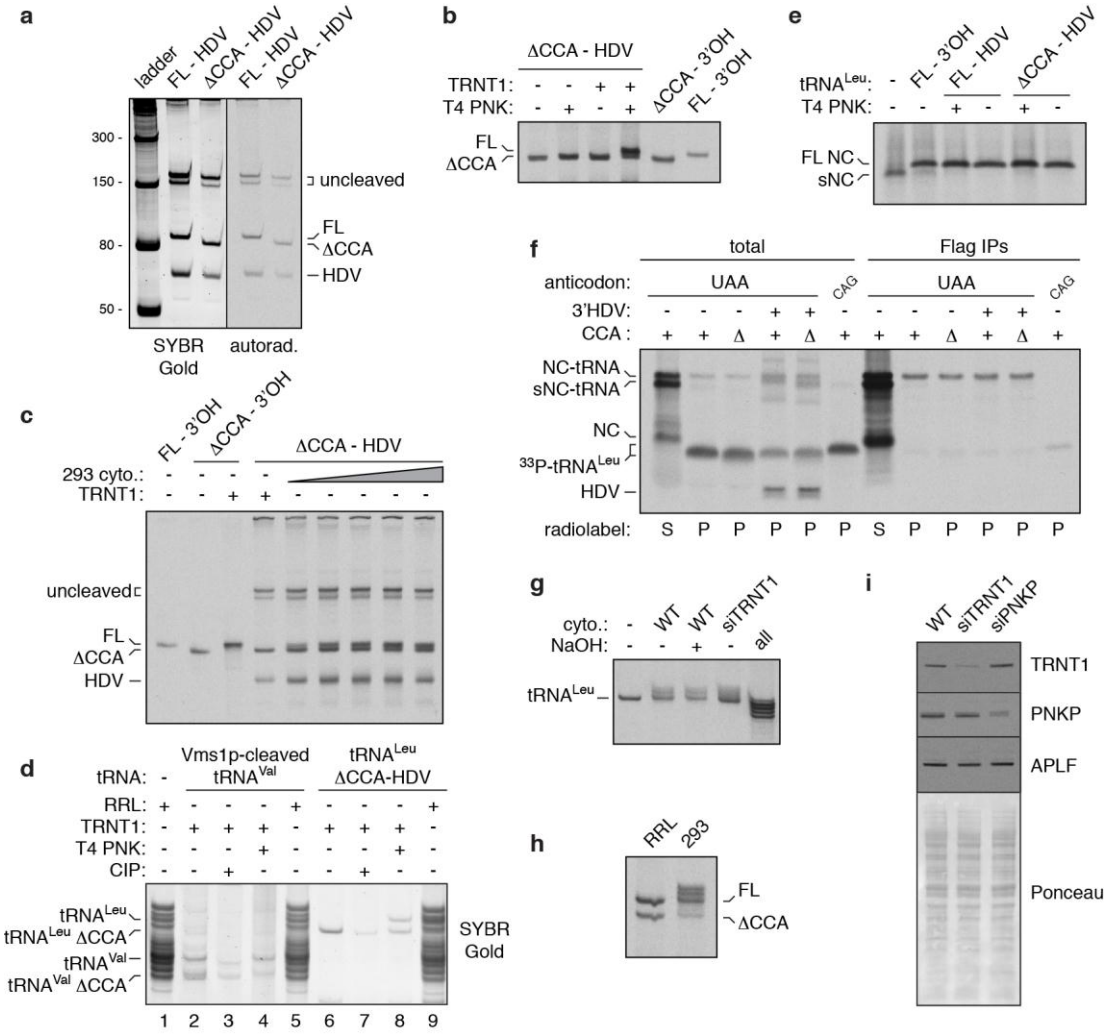

Supplementary Figure 8

tRNA recycling in mammalian cytosol.

a, TBE-urea-PAGE and SYBR Gold (left) or autoradiography (right) analysis of transcription reactions of full-length (FL-HDV) and ΔCCA tRNA^{Leu} (ΔCCA-HDV) constructs containing a 3' hepatitis delta virus (HDV) ribozyme (see Fig. 4a). The unprocessed, 5' tRNA fragments containing a 2',3'-cyclic phosphate, and 3' HDV fragments are indicated. **b,** Radiolabeled ΔCCA-HDV was treated with 0.12 U/μL T4 PNK followed by 100 nM TRNT1 as indicated in the presence of 0.1 mM NTPs. Note that, like Vms1p-cleaved tRNAs, CCA addition by TRNT1 only occurs after T4 PNK treatment. This contrasts with transcribed tRNAs, which are directly modified by TRNT1 (see Fig. 3a and Supplementary Fig. 7a). **c,** Radiolabeled ΔCCA-HDV was incubated with increasing amounts of hypotonic cytosolic lysate isolated from HEK293 cells and analyzed by TBE-urea-PAGE and autoradiography, demonstrating that recycling of ΔCCA-HDV to full-length (FL) tRNA^{Leu} is intact in these cytosolic lysates. **d,** SYBR Gold stain of the TBE-urea-PAGE gels analyzed by autoradiography in Fig. 4c. **e,** Cell-free translation reactions of an mRNA containing three rare UUA leucine codons in endogenous rabbit reticulocyte lysate supplemented with the indicated tRNAs, demonstrating that FL-HDV and ΔCCA-HDV rescue translation similarly as transcribed tRNAs with 3'-hydroxyl groups. **f,** Cell-free translation reactions of a truncated mRNA substrate ending in two rare UUA leucine codons (as in Fig. 2a). Reactions were in an endogenous rabbit reticulocyte lysate system with ^{35}S-methionine and no exogenous tRNAs, or with cold methionine and the indicated radiolabeled tRNAs. Reactions were directly analyzed by NuPAGE and autoradiography before (left) or after (right) immunoprecipitations (Flag IPs) against the N-terminal Flag tag encoded in the nascent protein. This demonstrates that the radiolabeled tRNAs are incorporated into ribosome-nascent protein complexes (RNCs). **g,** FL-HDV was incubated with the indicated 293 lysates at physiological or high pH (by addition of NaOH) to observe additional modifications. The high pH, which would hydrolyze amino acid-tRNA ester bonds, rules out the

possibility that the higher molecular weight bands are due to aminoacylation. **h,** ΔCCA-HDV was incubated with rabbit reticulocyte lysate (RRL) or HEK293 cytosol and directly analyzed by TBE-urea-PAGE and autoradiography, demonstrating a higher rate of additional modifications by HEK293 lysate. **i,** Immunoblotting and Ponceau stain analysis of cytosolic lysates isolated from HEK293T cells knocked down for the indicated proteins used in Fig. 4e. APLF is a control protein.

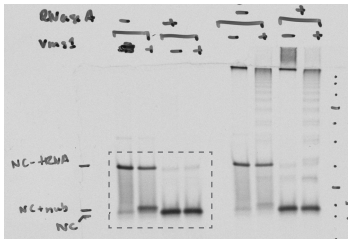

Fig. 1d

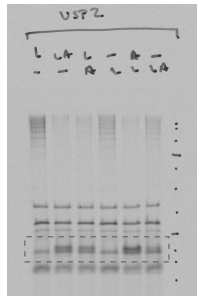

Fig. 1c

Fig. 3a

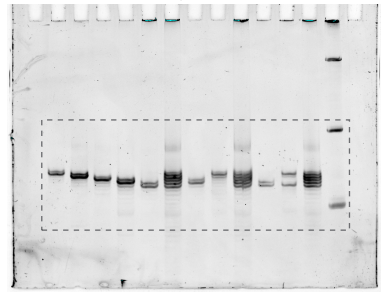

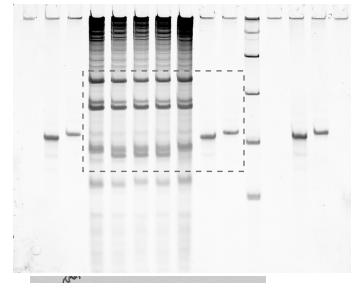

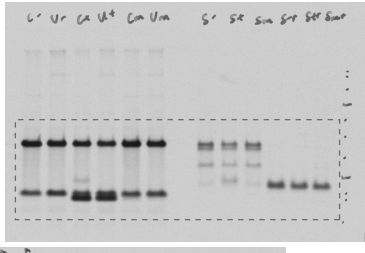

Fig. 2b

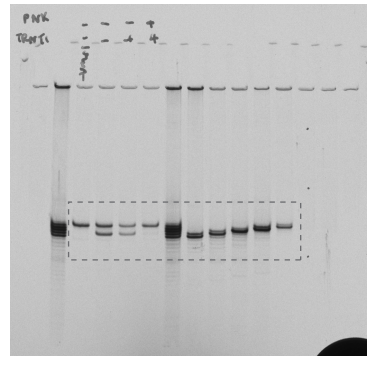

Fig. 3b

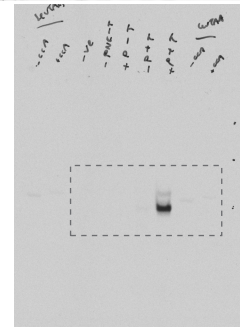

Fig. 3c

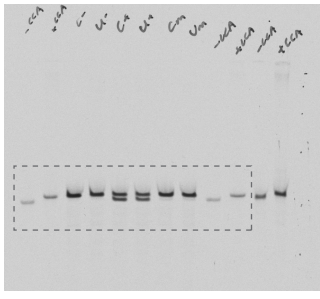

Fig. 2c

Fig. 4b

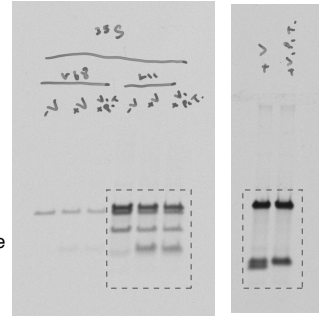

Fig. 3e

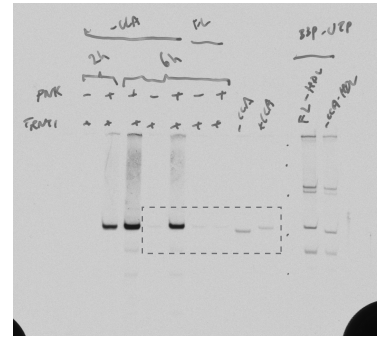

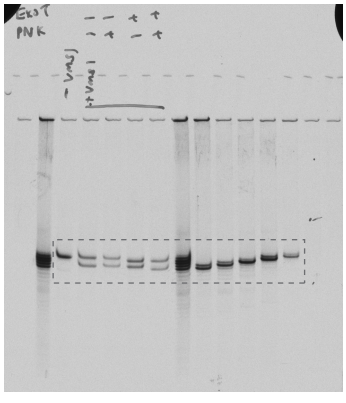

Fig. 2d

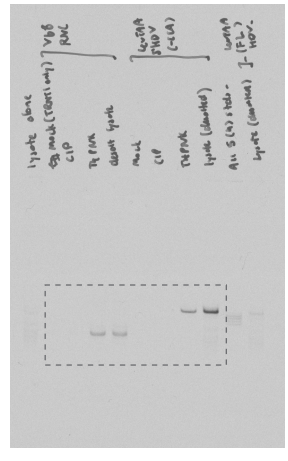

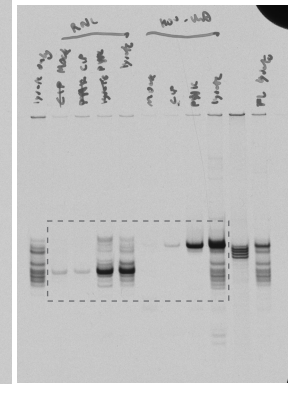

Fig. 4c

Fig. 4e

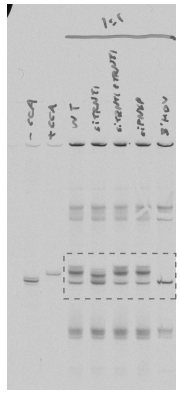

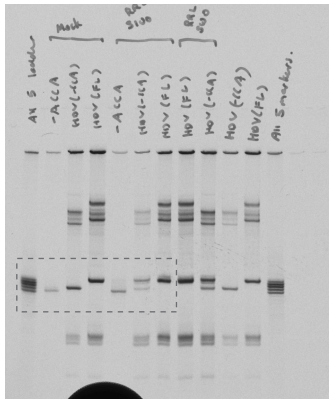

Fig. 4d

nature research

Corresponding author(s): Sichen Shao

Last updated by author(s): 2/26/19 (final submission)

Reporting Summary

Nature Research wishes to improve the reproducibility of the work that we publish. This form provides structure for consistency and transparency in reporting. For further information on Nature Research policies, see Authors & Referees and the Editorial Policy Checklist.

Statistics

For all statistical analyses, confirm that the following items are present in the figure legend, table legend, main text, or Methods section.

n/a	Confirmed	
☒	☐	The exact sample size (*n*) for each experimental group/condition, given as a discrete number and unit of measurement
☒	☐	A statement on whether measurements were taken from distinct samples or whether the same sample was measured repeatedly
☒	☐	The statistical test(s) used AND whether they are one- or two-sided *Only common tests should be described solely by name; describe more complex techniques in the Methods section.*
☒	☐	A description of all covariates tested
☒	☐	A description of any assumptions or corrections, such as tests of normality and adjustment for multiple comparisons
☒	☐	A full description of the statistical parameters including central tendency (e.g. means) or other basic estimates (e.g. regression coefficient) AND variation (e.g. standard deviation) or associated estimates of uncertainty (e.g. confidence intervals)
☒	☐	For null hypothesis testing, the test statistic (e.g. *F*, *t*, *r*) with confidence intervals, effect sizes, degrees of freedom and *P* value noted *Give P values as exact values whenever suitable.*
☒	☐	For Bayesian analysis, information on the choice of priors and Markov chain Monte Carlo settings
☒	☐	For hierarchical and complex designs, identification of the appropriate level for tests and full reporting of outcomes
☒	☐	Estimates of effect sizes (e.g. Cohen's *d*, Pearson's *r*), indicating how they were calculated

Our web collection on statistics for biologists contains articles on many of the points above.

Software and code

Policy information about availability of computer code

Data collection	No software was used
Data analysis	No software was used

For manuscripts utilizing custom algorithms or software that are central to the research but not yet described in published literature, software must be made available to editors/reviewers. We strongly encourage code deposition in a community repository (e.g. GitHub). See the Nature Research guidelines for submitting code & software for further information.

Data

Policy information about availability of data

All manuscripts must include a data availability statement. This statement should provide the following information, where applicable:

- Accession codes, unique identifiers, or web links for publicly available datasets
- A list of figures that have associated raw data
- A description of any restrictions on data availability

All data generated or analysed during this study are included in this published article (and its supplementary information files)

Field-specific reporting

Please select the one below that is the best fit for your research. If you are not sure, read the appropriate sections before making your selection.

☒ Life sciences ☐ Behavioural & social sciences ☐ Ecological, evolutionary & environmental sciences

For a reference copy of the document with all sections, see nature.com/documents/nr-reporting-summary-flat.pdf

Life sciences study design

All studies must disclose on these points even when the disclosure is negative.

Sample size	Our biochemical experiments are internally controlled and do not rely on sample size.
Data exclusions	No data were excluded
Replication	Attempts at replicating experiments in the manuscript were successful and described in figure legends. We performed at least 3 iterations of each representative experiment on different days to ensure results are reproducible.
Randomization	n/a - we did not have control vs. experimental groups in this biochemical study
Blinding	n/a - we did not have control vs. experimental groups in this biochemical study

Reporting for specific materials, systems and methods

We require information from authors about some types of materials, experimental systems and methods used in many studies. Here, indicate whether each material, system or method listed is relevant to your study. If you are not sure if a list item applies to your research, read the appropriate section before selecting a response.

Materials & experimental systems

n/a	Involved in the study
☐	☒ Antibodies
☐	☒ Eukaryotic cell lines
☒	☐ Palaeontology
☒	☐ Animals and other organisms
☒	☐ Human research participants
☒	☐ Clinical data

Methods

n/a	Involved in the study
☒	☐ ChIP-seq
☒	☐ Flow cytometry
☒	☐ MRI-based neuroimaging

Antibodies

Antibodies used	Antibodies against TRNT1 (Novus Biologicals NBP1-86589, lot A104178), PNKP (Novus Biologicals NBP1-87257, lot A115473), APLF (Proteintech 14252-1-AP), ANKZF1 (Santa Cruz sc-398713, clone B-12, lot H2614), and TOM20 (Santa Cruz sc-17764, clone F-10, lot F1417) were purchased and all used at a 1:1000 dilution.
Validation	Antibodies were validated by manufacturers via immunoblotting, immunofluorescence, and/or immunohistochemistry combined with genetic strategies and reexpression (TRNT1: https://www.novusbio.com/products/trnt1-antibody_nbp1-86589 immunoblotting with genetic strategies and 2 citations; PNKP: https://www.novusbio.com/products/pnk-antibody_nbp1-87257 immunoblotting, immunofluorescence, and immunohistochemistry with genetic strategies; APLF: https://www.ptglab.com/products/APLF-Antibody-14252-1-AP.htm with immunoblotting; ANKZF1: https://www.scbt.com/scbt/product/ankzf1-antibody-b-12 immunoblotting; TOM20: https://www.scbt.com/scbt/product/tom20-antibody-f-10 immunoblotting and immunostaining). We further validated antibodies by immunoblotting endogenous cell lysates with genetic knockdowns and/or with recombinant proteins (Sup. Fig. 7c, 8i).

Eukaryotic cell lines

Policy information about cell lines

Cell line source(s)	HEK293 and HEK293T cells were originally obtained from ATCC
Authentication	Cell lines were authenticated by STR profiling
Mycoplasma contamination	Cells were free of mycoplasma contamination; we routinely check all of our cell lines for mycoplasma contamination yearly.
Commonly misidentified lines (See ICLAC register)	No commonly misidentified cell lines were used.